Eye Movement Studies with a Vestibular Prosthesis

by Michael A. Saginaw

S.B. Electrical Science and Engineering, MIT, 1996
M.Eng. Electrical Engineering and Computer Science, MIT, 1997

Submitted to the Department of Electrical Engineering and Computer Science
in partial fulfillment of the requirements for the degree of

Doctor of Philosophy in Electrical Engineering
at the Massachusetts Institute of Technology

February 2010

Signature of Author: _____
Department of Electrical Engineering and Computer Science, MIT
December 8, 2009

Certified by: _____
Daniel M. Merfeld, Ph.D. – Thesis Supervisor
Associate Professor of Otolaryngology, Harvard Medical School

Accepted by: _____
Terry P. Orlando, Ph.D. – Graduate Officer
Professor of Electrical Engineering and Computer Science, MIT

Eye Movement Studies with a Vestibular Prosthesis

by – Michael A. Saginaw

Submitted to the Department of Electrical Engineering and Computer Science
on December 8, 2009 in partial fulfillment of the requirements
for the degree of Doctor of Philosophy in Electrical Engineering

Abstract

Vestibular loss, which can manifest as dizziness, imbalance, or spatial disorientation, is widespread and often caused by inner ear hair cell malfunction. To address these problems, we are developing a vestibular implant analogous to cochlear implants for the deaf. This vestibular prosthesis provides pulsatile electrical stimulation to the vestibular nerve. Prosthesis effectiveness is assessed using the vestibulo-ocular reflex (VOR), since the VOR helps stabilize gaze in healthy individuals by evoking eye movements that compensate for head movements.

In this thesis, the prosthesis was used to probe the high frequency VOR in squirrel monkeys and guinea pigs. In two studies, modulated stimulation was applied acutely to characterize the VOR between 1.5 and 701 Hz. A third study characterized the VOR response to chronic stimulation with a constant rate of 250 Hz.

The VOR has previously been characterized up to 50 Hz in monkeys and 2 Hz in guinea pigs by physically rotating subjects. This range was extended in these studies, by using electrical stimulation from the prosthesis. Eye movement spectral peaks were used to characterize the VOR frequency response. The VOR was measurable up to 267 Hz in squirrel monkeys and 151 Hz in guinea pigs. The magnitude response was similar in both species – it increased gradually with frequency, peaked (at 140 Hz in squirrel monkeys and 50 Hz in guinea pigs), and then rolled off. The high frequency fall-off was consistent with the low-pass nature of the oculomotor plant. The phase responses had a linear lag with frequency, consistent with a fixed 4 ms delay of the VOR three-neuron-arc.

Since the VOR responds at high frequencies, this raises the question whether the prosthesis causes eye movements at the prosthesis pulse rate, since electrical stimulation elicits neural responses that are phase-locked with the stimulation. Such responses might cause visual blurring for a patient using the device. This thesis shows that such eye movements are measurable, and have substantial velocity magnitude of 8.1 deg/s initially, but within 30 minutes the magnitude reduces by 80% and probably does not yield perceptible visual blurring.

Thesis Supervisor: Daniel M. Merfeld
Title: Associate Professor of Otolaryngology, Harvard Medical School

Table of Contents

Chapter 1. Introduction

Vertigo and imbalance are commonly occurring problems. Vestibular vertigo affects approximately 5% of adults each year (Neuhauser et al. 2005), and can be a life-altering problem. Furthermore, people who report dizziness are 12 times more likely to experience falls (Agrawal et al. 2009), which are a leading cause of severe health problems.

Chronic vestibular vertigo can be caused by malfunction of inner ear hair cells due to aging, or due to damage by certain antibiotics. It can also be caused by Meniere's syndrome, which might be the result of endolymphatic hydrops or autoimmune disease. In the Jenks Vestibular Physiology Laboratory at the Massachusetts Eye and Ear Infirmary, we are developing a prosthesis to alleviate these problems. The prosthesis is analogous to a cochlear implant for the deaf. Our prosthesis bypasses vestibular hair cells and electrically stimulates the vestibular nerve, providing information about the subject's head motion.

Vestibular Prosthesis Design

The prosthesis design is based on research that has elucidated how the vestibular system works. When the head moves, the bony walls of the semicircular canals move with it, but the endolymph fluid within the canals lags the head motion, and presses against the cupula membranes, which largely seal each canal ampulla. The cupula deforms, by an amount proportional to head angular velocity at physiological rotation frequencies, and bends the cilia that are embedded in it. This modulates the firing rate that the hair cells produce on the vestibular nerve. At physiologic frequencies the firing rate changes roughly linearly above or below the spontaneous rate (the rate when the head is not turning), in proportion to head angular velocity (Fernandez and Goldberg 1971, Goldberg and Fernandez 1971).

Vestibular dysfunction can disrupt this transduction process; therefore, the prosthesis is designed to bypass it. In the prosthesis, an angular rate sensor detects head angular velocity. This signal is sent to a microprocessor which modulates the rate of current pulses that are delivered via an electrode to the vestibular nerve. The prosthesis is currently being tested in laboratory animals. All work with laboratory animals adheres strictly to a protocol approved by the Institutional Care and Use Committee of the Massachusetts Eye and Ear Infirmary, and complies with the guidelines of the National Institutes of Health. All surgeries use aseptic techniques, and all implanted materials are biocompatible.

Eye Movement Studies in this Thesis

The prosthesis is assessed by measuring eye movements, since the vestibulo-ocular reflex (VOR) helps maintain steady gaze as the head moves. The angular VOR has been previously studied up to 2 Hz in guinea pigs (Escudero et al. 1993, Andrews et al. 1997, Pettorossi et al. 1986), 15 Hz in squirrel monkeys (Minor et al. 1999), and 50 Hz in rhesus monkeys (Ramachandran and Lisberger 2005), by physically rotating subjects.

The gain is near 1 up to 20 Hz, and then increases to near 3 by 50 Hz. The phase is compensatory for motion up to 25 Hz, but lags head motion at higher frequencies.

These findings raise questions about how the VOR behaves at higher frequencies. Does the gain ultimately fall off, due to the low-pass nature of the oculomotor plant? Does the phase lag continue, and can it be related to the latency of the VOR? However, it is difficult to use physical rotation to provide higher frequency stimulation with controlled spectral content.

In this thesis, the vestibular prosthesis was used to study the angular VOR in awake guinea pigs and squirrel monkeys at higher frequencies, using electrical stimulation. Since VOR responses were indeed measurable above 100 Hz, this raises the question whether the pulsatile stimulation from the prosthesis causes eye movements at the stimulation pulse frequency, since electrical stimulation of neurons causes phase-locked responses (Kiang and Moxon 1972). Could the prosthesis cause blurry vision, even while stabilizing an individual's sensation of spatial orientation?

The studies in this thesis were developed around three specific aims in a funded NIH F31 predoctoral fellowship:

Specific Aim 1: Characterize the angular VOR frequency response in awake guinea pigs and squirrel monkeys from 1.5 to 701 Hz, using electric stimulation

> *Hypothesis*: The magnitude response will fall off above 100 Hz, due to the low-pass nature of the oculomotor plant. The phase response will have a linear lag as a function of frequency, due to the fixed response delay of the VOR.

Specific Aim 2: Study whether pulsatile electric stimulation of the vestibular nerve elicits eye movements at the stimulation pulse frequency

> *Hypothesis*: There will be an eye movement component at the stimulation pulse frequency

Specific Aim 3: Study whether the eye movements at the stimulation pulse frequency reduce over time

> *Hypothesis*: Over time, the eye movement component will reduce and become imperceptible

Organization of Thesis

Chapter 2 describes the frequency response of the angular VOR in the squirrel monkey, in response to electric stimulation of the peripheral vestibular nerve. Stimulation ranged from 1.5 to 701 Hz. The magnitude response was fairly flat up to 5 Hz, fell until 20 Hz, rose to a peak near 140 Hz, and then rolled off at higher frequencies, consistent with the low-pass nature of the oculomotor plant. The phase response had a linear lag with frequency, consistent with a 4 ms constant delay of the three-neuron arc of the VOR. Control studies verified that the response was physiological, rather than artifactual, up

to 267 Hz. Thus, the nervous system was capable of conveying signals and eliciting VOR eye movements above 200 Hz.

Chapter 3 describes the high frequency angular VOR in the guinea pig. Stimulation ranged from 1.5 to 293 Hz. The magnitude responses were similar in overall shape to those in the squirrel monkey, but peaked at a lower frequency of 50 Hz. This may have been due to different characteristics of the oculomotor plant, perhaps related to slower eye movement requirements in the guinea pig. The VOR was found up to 151 Hz in these studies in the guinea pig. The phase response had a linear lag as a function of frequency, consistent with a 4 ms constant delay, similar to the squirrel monkey.

A major result of chapters 2 and 3 is that the VOR is found at high frequencies, well above 100 Hz in guinea pigs and 200 Hz in squirrel monkeys. This raises the question whether the prosthesis will cause substantial eye movements at the stimulation pulse rate. Such eye movements might cause visual blurring.

Chapter 4, therefore, describes a study of guinea pig eye movements at 250 Hz, when stimulation at 250 pulses/s was delivered chronically. Indeed there was a clear 250 Hz eye movement component, with a velocity magnitude of 8.1 deg/s when stimulation was turned on. However within half an hour the component reduced to 1.6 deg/s (with a time constant of 5.0 minutes), corresponding to peak-to-peak position changes of 7.3 arcsec, which would probably be imperceptible. Thus eye movements phase-locked to the prosthesis stimulation do not appear to pose a serious long-term problem.

However, this phenomenon may impose a constraint on the lower limit for the baseline pulse rate when the prosthesis is used in humans. If humans have a VOR magnitude response similar to squirrel monkeys, with a peak around near 140 Hz, then the prosthesis baseline pulse rate may need to be well above that in order to minimize or prevent visual blurring.

With respect to publication plans, chapters 2 and 3 will be submitted to the Journal of Neurophysiology. Chapter 4 will be submitted to the IEEE Transactions on Biomedical Engineering.

Chapter 5 concludes by summarizing the main findings of the thesis. It also revisits the low frequency VOR phase responses of chapters 2 and 3, and explores the effect of the stimulation biphasic pulse rate. Linear system modeling is used to explain those results in terms of the oculomotor neural integrator, which transforms velocity signals into a motor command that controls eye position.

Contributions of Thesis

These studies extend scientific knowledge of the high frequency VOR by using the prosthesis as a tool, and explore clinically-motivated questions about the impact of prosthesis stimulation on visual quality to provide a better understanding of the likely outcome when the prosthesis is used in awake human patients. They are the first characterization of the VOR magnitude and phase responses above 50 Hz. There are five main contributions:

- High Frequency VOR Magnitude Response: Prior work using physical rotation has shown an increase in the VOR gain from 20 to 50 Hz in monkeys. However, the oculomotor plant has strongly low-pass characteristics, suggesting that the magnitude response must fall off at higher frequencies. These studies use electrical stimulation to probe higher frequencies, and show that the response does indeed fall off, above 140 Hz in squirrel monkeys (chapter 2) and above 50 Hz in guinea pigs (chapter 3).

- High Frequency VOR Phase Response: Prior work has shown that while the VOR phase response is compensatory for motion at low frequencies, there is a phase lag from 25 to 50 Hz. This raises the question whether the phase lag is due to the fixed delay of the VOR. These studies show the phase lag up to 267 Hz, and it is quite consistent with a fixed delay of 4 ms in both squirrel monkeys (chapter 2) and guinea pigs (chapter 3).
- Modeling: The high frequency roll-offs in the magnitude responses, the linear lags vs. frequency in the phase responses, and the low frequency phase leads in both squirrel monkeys and guinea pigs were all in agreement with the behavior predicted by linear system modeling of the oculomotor plant and central processing (chapters 2 and 3). For the mid-frequency magnitude response peaks, the fits were improved when the same model was altered to combine the two high frequency poles in a resonant pair.
- Eye Movements at Prosthesis Pulse Frequency: This thesis shows that VOR responses are found well above 100 Hz, which raises the question whether electric stimulation from a vestibular prosthesis will elicit eye movements at the stimulation pulse frequency, since electric stimulation elicits neural responses that are phase-locked to the stimulation. These studies show that such a component does occur when stimulation is turned on, but its magnitude reduces in just half an hour to a level that is unlikely to be perceptible to a human patient using the prosthesis (chapter 4).
- Spectral Analysis of Eye Movements: In these studies, various methods were tried for spectral analysis of eye movements (chapter 2):
  - Results were substantially improved when saccade and blink artifacts were excluded, since they were found to have a large effect on the low frequency spectrum, and some effect up to 160 Hz
  - Results were also substantially improved when spectra from different segments were combined using the averaged complex spectrum, i.e. a complex Cartesian average, rather than a magnitude-only and a phase-only average

References

Agrawal Y, Carey JP, Della Santina CC, Schubert MC, Minor LB. Disorders of balance and vestibular function in U.S. adults: data from the national health and nutrition examination survey, 2001-2004. *Arch Intern Med*, 169: 938-944, 2009.

Andrews JC, Koyama S, Li J, Hoffman LF. Vestibular and optokinetic function in the normal guinea pig. Ann Otol Rhinol Laryngol 106: 838-847, 1997.

Escudero M, de Waele C, Vibert N, Berthoz A, Vidal PP. Saccadic eye movements and the horizontal vestibulo-ocular and vestibulo-collic reflexes in the intact guinea-pig. *Exp Brain Res* 97: 254-262, 1993.

Fernandez C, Goldberg JM. Physiology of peripheral neurons innervating semicircular canals of the squirrel monkey. II. Response to sinusoidal stimulation and dynamics of peripheral vestibular system. *J Neurophysiol* 34: 661-675, 1971.

Goldberg JM, Fernandez C. Physiology of peripheral neurons innervating semicircular canals of the squirrel monkey. I. Resting discharge and response to constant angular accelerations. *J Neurophysiol* 34: 635-660, 1971.

Kiang NY, Moxon EC. Physiological considerations in artificial stimulation of the inner ear. *Ann Otol Rhinol Laryngol* 81: 714-730, 1972.

Minor LB, Lasker DM, Backous DD, Hullar TE. Horizontal vestibuloocular reflex evoked by high-acceleration rotations in the squirrel monkey. I. Normal responses. *J Neurophysiol* 82: 1254-1270, 1999.

Neuhauser HK, von Brevern M, Radtke A, Lezius F, Feldmann M, Ziese T, and Lempert T. Epidemiology of vestibular vertigo: a neurotologic survey of the general population. *Neurology* 65: 898-904, 2005.

Pettorossi VE, Bamonte F, Errico P, Ongini E, Draicchio F, and Sabetta F. Vestibulo-ocular reflex (VOR) in guinea pigs. *Acta Otolaryngol* 101: 378-388, 1986.

Ramachandran R., Lisberger SG. Normal performance and expression of learning in the vestibulo-ocular reflex (VOR) at high frequencies. *J Neurophysiol* 93: 2028-2038, 2005.

Chapter 2

Angular Vestibulo-Ocular Reflex Above 100 Hz Elicited by Electrical Stimulation of the Vestibular Peripheral Nerve. I. Responses in the Squirrel Monkey

Saginaw, Michael A.[1,2]
Gong, Wangsong[2,3]
Haburcakova, Csilla[2,3]
Merfeld, Daniel M.[2,3]

1. Department of Electrical Engineering and Computer Science, Massachusetts Institute of Technology, Cambridge MA

2. Jenks Vestibular Physiology Laboratory, Massachusetts Eye and Ear Infirmary, Boston MA

3. Department of Otology and Laryngology, Harvard Medical School, Boston MA

Abstract

The angular vestibulo-ocular reflex (VOR), which stabilizes gaze during head motion, has previously been characterized up to 50 Hz by physically rotating subjects. To study the VOR at higher frequencies, we electrically stimulated the peripheral vestibular nerve in awake squirrel monkeys. Stimulation consisted of biphasic charge-balanced pulses that were gated on or off by square wave modulation. The modulation frequency was varied from 1.5 to 701 Hz to obtain the frequency response. Spectral responses were computed using the fast Fourier transform. The VOR response was physiological and neurally conveyed, up to 267 Hz, as confirmed by control studies using anesthesia and euthanasia. The VOR magnitude response was constant within an order of magnitude from 1.5 to 150 Hz. It was fairly flat up to 5 Hz, decreased to a low near 20 Hz, increased to a peak near 140 Hz, and decreased at higher frequencies, in agreement with the high frequency fall-off expected from Robinson's fourth order mechanical model of the eye. The phase response had a clear lag as a function of frequency, consistent with a 4 ms pure delay of the simple VOR. We concluded that the nervous system is capable of conveying modulated signals above 250 Hz, and that eye movements can be evoked at these frequencies, even though the oculomotor plant is strongly low-pass. Both the magnitude and phase responses were consistent with signals at these high frequencies being transmitted by the simple VOR three-neuron arc.

Introduction

The vestibular system senses head motion and generates compensatory eye movements in order to help stabilize gaze. This response is known as the vestibulo-ocular reflex (VOR). In particular, angular head motion is sensed by the semicircular canals, which evoke the angular VOR. Previous studies have characterized the angular VOR as a function of frequency in squirrel monkeys and rhesus monkeys up to 50 Hz (Paige 1983a; Huterer and Cullen 2002; Minor et al. 1999; Ramachandran and Lisberger 2005). They found that the gain is near 1 up to 20 Hz, and increases towards 3 at higher frequencies. The phase is compensatory for head motion up to 25 Hz, and lags head motion at higher frequencies.

It is interesting to study higher frequencies of the angular VOR for several reasons. First, vestibular peripheral neurons have a maximum firing rate of about 400 spikes/s (Goldberg and Fernandez 1971). This raises the question whether it is possible that the VOR extends to similar frequencies. Second, VOR adaptation to visual cues appears ineffective above 25 Hz (Ramachandran and Lisberger 2005), thus studying the VOR at higher frequencies may reveal the behavior of the part of the reflex that does not adapt. Third, neural vestibular prostheses use high frequency electrical stimulation (Gong and Merfeld 2002; Della Santina et al. 2007). The prosthesis baseline rate might be designed to be about 200 pulses per second (pps), well above the mean peripheral spontaneous rate, in order to allow a unilateral prosthesis to provide bidirectional motion cues above the spontaneous rate. The modulated prosthesis output often extends above 300 pps, so it is important to characterize the VOR up to these frequencies.

Electrical stimulation offers several advantages for studying the high frequency VOR. First, it is very difficult to provide sinusoidal physical rotation above 50 Hz, but using electrical stimulation it is feasible to provide high frequency stimulation that is spectrally clean and carefully controlled. Second, electrical stimulation provides an opportunity to bypass the dynamics of the periphery, which facilitates the study of central mechanisms such as compensation (Skavenski and Robinson 1973; Robinson 1981). Finally, electrical stimulation allows studies to be carried out with the head remaining stationary. There has been some debate whether head motion above 8 Hz causes artifactual passive eye movements in the eye orbits (Vercher et al. 1984), confounding results from the VOR.

There are factors that might limit the maximum frequency at which an electrically evoked VOR can be evoked. First, the oculomotor plant is strongly low-pass. Second, the peripheral vestibular nerve units have a maximum firing rate of 400 spikes/s (Goldberg and Fernandez 1971). VOR responses above 400 Hz could only occur if parallel pathways were stimulated asynchronously. We hypothesized that the magnitude response would fall off above 100 Hz. For the high frequency VOR phase response, we hypothesized that it would lag linearly with frequency, due to the latency of the three-neuron arc of the simple VOR.

As part of a project to develop a vestibular implant, analogous to cochlear implants for the deaf, we used electrical stimulation to elicit eye movements at much higher frequencies than previously studied. Here, the angular VOR response was characterized from 1.5 to 701 Hz in the squirrel monkey. In a companion paper (Saginaw et al. 2009), the VOR was characterized in the guinea pig.

Methods

ANIMAL PREPARATION

Three mature (> 700 g) male squirrel monkeys (*Saimiri sciureus*), designated as monkeys "R", "G", and "N", were used as subjects. All work with animals adhered to a protocol approved by the Institutional Animal Care and Use Committee of the Massachusetts Eye and Ear Infirmary. During all surgeries, animals were under Isoflurane general anesthesia, and sterile instruments and materials were used. Surgical procedures included: (1) attaching a head bolt to the skull to secure a head cap on top of the monkey's head, (2) implanting a coil on the eye to measure eye position, (3) plugging both lateral semicircular canals to prevent modulation of the vestibular nerve signal by yaw head rotation, and (4) implanting electrodes to stimulate the vestibular system. Surgeries and instrumentation were similar to procedures described elsewhere (Gong and Merfeld 2000; Gong and Merfeld 2002, Merfeld et al. 2007, Gong et al. 2008), so only a brief description is provided.

The head bolt, made of a composite ("G10") and machined to shape, was attached to the skull using inverted titanium screws and dental acrylic, which also covered the opened area. The head bolt was used to securely hold the head cap, which was a small G10 box roughly 44 mm x 34 mm x 33 mm that housed electrode leads and electronics.

Eye coils were approximately 11 mm in diameter and consisted of three turns of stainless steel Cooner Wire AS632 (Cooner Wire, Inc., Chatsworth, CA). The coils were implanted frontally using standard methods (Judge et al. 1980). Eye coil leads were brought subcutaneously to the top of the head near the head cap. After a recovery period of at least 14 days, the monkeys with a head bolt and eye coil were tested using sinusoidal motion profiles, and eye movements were measured to verify normal VOR responses.

Both lateral semicircular canals were plugged in all monkeys, following standard methodology (Lasker et al. 1999). An incision was made in the skin behind each ear, and a hole was drilled through the bony wall of the canal labyrinth. Fascia and bone wax were inserted to plug the interior of the canal. Over time, ossification further secures the canal plugs. Canal plugging does not affect the experiments described here, because the monkeys were stationary and canal plugging does not affect the spontaneous rate of vestibular afferents (Paige 1983b, Lasker et al. 1999). Some degree of canal obstruction forms over time around the inserted electrodes (B. Silveira, unpublished observations), and the status of the canals is made definite by plugging them. Also, canal plugging was done because these monkeys were used in other studies that did involve motion stimuli.

All monkeys had electrodes implanted bilaterally. An incision was made in the skin behind each ear, and a small hole was drilled in the bony wall of the lateral canal near the ampulla. A Teflon coated platinum electrode, made from 150 μm diameter Cooner Wire AS770-40, was inserted near the nerve branch innervating the ampulla of the lateral canal. Prior to insertion, Teflon insulation was removed to expose 100-200 μm of platinum wire. Additional details on the electrode are described elsewhere (Gong and Merfeld 2000). The electrode position was adjusted, using a micromanipulator, until electrical stimulation elicited eye movements that were predominantly horizontal, as monitored visually. The hole was then sealed with bone wax and the electrode was fixed in place with stainless steel screws and dental acrylic. The return electrode, made of the same kind of platinum wire with about 2 mm of insulation stripped, was inserted superficially into muscle near the operated ear. Electrode leads were brought subcutaneously to the top of the head near the head cap, making them inaccessible to

the monkey. Following ear surgeries, the monkeys were allowed to recover for at least 14 days before testing. For monkeys "R" and "G", only one electrode was viable at the time of testing; for monkey "N", tests were done on both ears.

VOR Frequency Response Tests

During experiments the monkeys were stationary, seated upright in a custom fabricated chair. The chair held the head cap, and painlessly fixed the head position at a forward pitch angle of approximately 15°, in order to bring the lateral canals approximately parallel with earth-horizontal. The chair positioned the monkey so that its eyes were near the center of the frame of the search coil system. Experiments were conducted in the dark, in order to focus on vestibular-driven eye movements. Since squirrel monkeys fall asleep in the dark, we used low dose d-amphetamine (0.3 mg/kg IM) to keep them awake during testing. In a previous study (Paige 1983a), d-amphetamine did not have a different effect on the VOR than the use of liquid reward as a way to maintain alertness in squirrel monkeys in the dark.

Electrical stimulation was delivered to the electrode implanted in the ampulla of the lateral canal. Stimulation consisted of a pattern of charge-balanced biphasic pulses. We used a current source stimulator to control charge delivery because that is the most important parameter determining the effectiveness of neural stimulation (Mortimer 1990). A voltage source stimulator would deliver unpredictable charge due to changes in tissue impedances over time (Babb et al. 1977; Shepherd et al. 1990). We used charge balanced pulses to reduce electrode dissolution (Robbee and Rose 1990).

Each biphasic pulse was composed of a negative (cathodic) current pulse lasting 50 μs, followed immediately by a positive (anodic) current pulse, also lasting 50 μs. For each monkey, the current amplitude was chosen to be large enough to elicit eye movements, but small enough to not stimulate the facial nerve to cause facial twitching. We used 200 μA for monkeys "R" and "G", and 300 μA for monkey "N". These were below the charge delivery levels used in other experiments with long-term stimulation (Merfeld et al. 2007; Gong et al. 2008).

The stimulation pattern consisted of biphasic pulses in a constant, high-rate pulse train that was modulated by a square wave, which gated the pulse train on or off. With square waves we could stimulate many frequencies simultaneously. This allowed us to keep the total stimulation duration short, and we did not want to pre-adapt these monkeys since they were subsequently used in chronic stimulation studies. Also, square waves only stimulate at one current amplitude, which would have simplified our stimulation in case the system were significantly nonlinear.

Monkeys "R" and "G" were tested with a biphasic pulse rate of 5000 pps, which allowed us to use a wide range of modulation frequencies and still maintain many biphasic pulses in each "on" portion of the modulation. Modulation frequencies ranged from 1.5 to 701 Hz. All three monkeys were also tested with a biphasic pulse rate of 250 pps and modulation frequencies from 1.5 to 123 Hz.

The modulation frequencies included more than 20 values from 1.5 to 701 Hz inclusive and were spaced approximately logarithmically. A few modulation frequencies were deliberately chosen as multiples of other modulation frequencies, e.g. 9 Hz was used in order to compare its results to those from the 3rd harmonic of 3 Hz, which was also a modulation frequency. However, most modulation frequencies were selected as

prime numbers, to preclude possible interferences (e.g. 30 Hz was not chosen, to preclude possible confounding effects of the 60 Hz power system)[1].

Stimulation duration was 10 seconds, but for modulation frequencies below 10 Hz the stimulation duration was 30 seconds in order to include enough data for analysis. These durations were kept short in order to prevent acclimation (Merfeld et al. 2006).

Eye position was measured using a Robinson (Robinson 1963) style search coil system (C-N-C Engineering, Seattle WA) with coil frequencies of 72 kHz and 108 kHz. The coil system's phase detector outputs were filtered for anti-aliasing by 5^{th} order Bessel low pass filters with a -3dB frequency of 3000 Hz, and recorded at 12 kHz[2] or 20 kHz. Sampling was done with a 16 bit analog-to-digital converter with a resolution of 320 μV per bit (which corresponded to approximately 640 μdegrees/bit), on a data acquisition card controlled by LabView (both by National Instruments, Austin TX).

Control Tests and Artifacts

Control tests were necessary to show that recorded eye signals were not artifacts. One monkey's ear electrode was stimulated and the eye coil signal was measured as in normal tests. For anesthesia tests, the monkey was given 15 mg/kg pentobarbital intramuscularly, and for a euthanasia test, the monkey was given 110 mg/kg pentobarbital intravenously. For these control tests, d-amphetamine was not used.

Data Analysis

Data processing and spectral analysis were carried out in MATLAB (The MathWorks, Natick MA). Eye movement spectra were computed using fast Fourier transforms of non-overlapping segments of eye position data. Segments were 1 second for modulation frequencies below 10 Hz, in order to include more than one cycle. For higher modulation frequencies, segments were ½ second in order to provide enough windows for averaging. Segments were processed to remove the linear trend, since squirrel monkeys typically have a small spontaneous nystagmus. Data segments were then tapered by Hann windows to reduce spectral leakage from e.g. components at power harmonic frequencies. For the spectra, velocity was calculated in the frequency domain via multiplication by a frequency ramp. Spectra were scaled so that a magnitude of 1 corresponded to a time-domain velocity signal of 1°/s in amplitude at 1 Hz (scaling included normalizing out the Hann window's effect on spectral magnitude, by using the sum of the taps of the Hann window's impulse response). For each data segment, the phase of the eye movements was computed as the phase of the segment's Fourier transform minus the phase of the Fourier transform of the stimulation in the same data segment.

Spectra are shown in figure 2.1, for an experiment using 5000 pps and 3 Hz modulation with monkey "G". Figure 2.1A shows the spectral magnitude of the stimulation. This spectrum has peaks at all odd harmonics of the modulation frequency, and their magnitudes scale inversely with frequency. This is expected, because the stimulation is formed by multiplying the biphasic pulse train by the modulating square

---

[1] Modulation frequencies for monkey "R" were 1.5, 2, 3, 5, 7, 9, 13, 31, 53, 73, 123, 149, 199, 293, 317, 503, and 701 Hz. Additional modulation frequencies used with monkey "G" were 21, 41, 65, 89, and 233 Hz.

[2] The sampling rate was very close to 12 kHz. The data acquisition hardware was limited to integer multiples of its 50 ns clock, and we used the true sampling interval of 83.35 μs (~11.9976 kHz) in data analysis.

wave. This multiplication in the time domain corresponds to convolution in the frequency domain. Since the square wave spectrum consists of components at the odd harmonics of the square wave's fundamental frequency, these odd harmonics appear in the spectrum of the stimulation. Figure 2.1B shows the spectral magnitude of the horizontal eye velocity. The magnitude spectra from different time windows were averaged to reduce variance in the spectral estimate, as is typical in spectral analysis (Oppenheim et al. 1999). For a linear system we would expect the response to have spectral peaks at the same frequencies as the stimulation. The response spectrum does indeed have slight peaks at 3 Hz and 9 Hz. However it has a long, large tail which obscures peaks at higher harmonics. Two factors contributed to the tail: nystagmic quick phases, and the bias of averaging only the spectral magnitudes. When both of these factors were removed, the improvements in figure 2.1C were obtained.

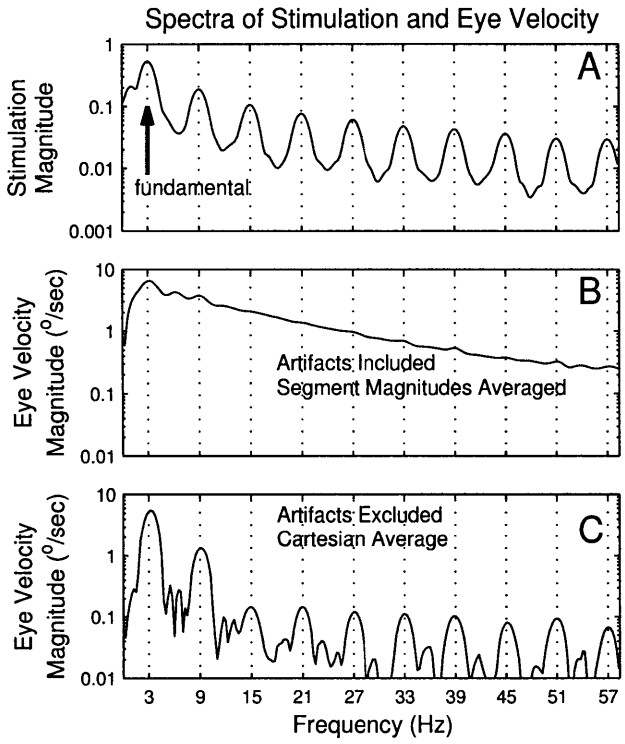

Figure 2.1. Magnitude spectra from experiments with 3 Hz modulation. (A) Spectrum magnitude of the stimulation recorded during the experiment. As expected from spectral theory (since multiplication by a modulating square wave in the time domain corresponds to convolution in the frequency domain), the square wave modulation at 3 Hz produces spectral lines at odd harmonics of the modulation frequency, and the spectral line strengths vary inversely with frequency. (B) Horizontal eye velocity spectrum magnitude. Nystagmic quick phases and blinks were included in the time-domain data segments that were used to compute the spectra. Also, segment spectral magnitudes were averaged to form the spectrum magnitude shown. (C) Improved method for computing horizontal eye velocity spectrum magnitude. Quick phases and blinks were excluded, and segment spectra were combined using an averaged complex spectrum (Cartesian average). These techniques reduced low frequency noise and revealed peaks at a large number of odd harmonics, as would be expected for stimulation with square wave modulation. Therefore these techniques were used for all other spectral calculations and plots.

In order to remove quick phases and blinks, they were marked in the time plots and excluded from spectral calculations. Since quick phases are step-like signals, they add significant noise at low frequencies and less noise at high frequencies. When quick phases and blinks were excluded, there was a reduction in the spectral noise floor from low frequencies up to 160 Hz in the squirrel monkey. Above 160 Hz, there was typically no difference in the noise floor whether or not quick phases and blinks were excluded. The exclusion of quick phase and blink artifacts also reduced the number of usable data

segments; however, there were still a minimum of 11 data segments for each experiment at 5000 pps. For experiments at 250 pps, data from a given modulation frequency was only used when there was a minimum of 5 usable data segments available for averaging.

In order to eliminate the bias, the averaged complex spectrum was used instead of just averaging the magnitudes. The complex spectra from each segment were averaged, and from that Cartesian average, the magnitude was computed. All four combinations of processing were tried – including vs. excluding artifacts; and using the magnitude-only average vs. using the Cartesian average. The processing outcome was substantially improved by excluding artifacts and using the Cartesian average. In figure 2.1C, a large number of higher harmonics are clearly visible in the spectrum. Since these higher harmonics are clear peaks above the surrounding noise floor, the higher harmonics can be used in addition to data at the fundamental frequency.

Results

VOR Frequency Response Tests with 5000 pps

Time plots in figure 2.2 show eye movements in response to electrical stimulation at 5000 pps. The square wave patterns at the bottom of the plots indicate when stimulation was applied. There was little eye movement activity prior to stimulation. Once stimulation commenced, the eye movements were clearly phase-locked to the modulated stimulation. With 2 Hz modulation, horizontal eye movements at 2 Hz were clearly visible (figure 2.2A).

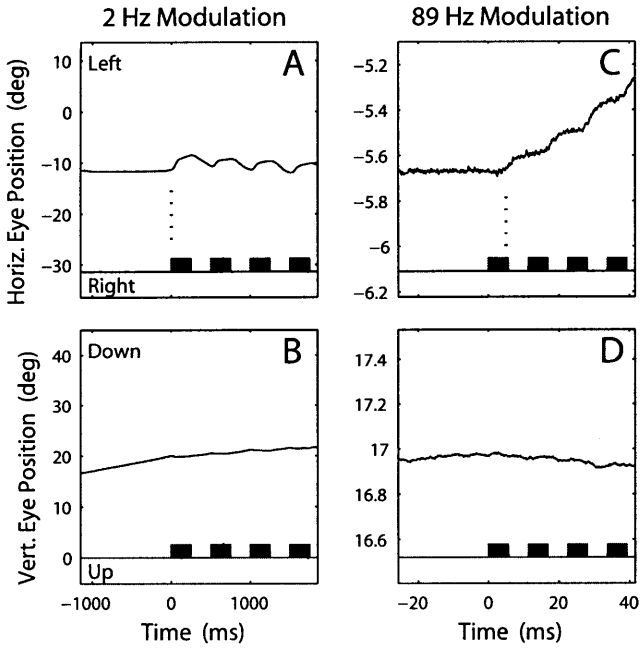

Figure 2.2. Time plots of eye position in response to electrical stimulation for squirrel monkey "G". The square wave patterns near the bottom of the plots indicate the time when stimulation was given. (A) and (B) show an experiment with 2 Hz modulation. Stimulation in the right ear caused slow phase eye movements to the left, as expected. The effect was much greater in horizontal eye movements (A) compared to vertical eye movements (B), as expected, because the electrode was inserted in the ampulla of the lateral canal during surgery. (C) and (D) show an experiment with 89 Hz modulation. In (C) the latency between stimulation onset and eye movements is clearly visible, indicated by the dotted lines at 5 ms.

Similarly, for 89 Hz modulation, horizontal eye movements at 89 Hz were clearly visible (figure 2.2C). For the 89 Hz case, the x-scales are zoomed in (to show the same number of modulation cycles as for the 2 Hz case), and on this time scale there is also a clearly visible latency of about 5 ms between onset of stimulation and the first eye response. Horizontal eye movements (figure 2.2A and 2.2C) were much more evident than vertical eye movements (figure 2.2B and 2.2D), as expected since the electrode was placed in the lateral canal.

Figure 2.3 compares spectral responses at the fundamental modulation frequency to responses at higher harmonics. The higher harmonics are present because the stimulation was modulated by a square wave. Since multiplication in the time domain corresponds to convolution in the frequency domain, the odd harmonics of the square wave frequency appeared in the spectrum of the stimulation, and the strength of those components varied inversely with frequency. Accordingly, figure 2.3A shows monkey "G" eye movement responses at the fundamental modulation frequency, as well as at the 3rd and 5th harmonics of the modulation frequency, and these are scaled up by factors of 3 and 5 respectively, to make them comparable to the response at the fundamental frequency. These harmonics were only included if they had a clear peak above the surrounding noise floor, judged by eye. Also, only harmonics that were 267 Hz or below were included, as these results avoid artifacts (see description of control test results). Responses from all these harmonics were consistent with each other – for all harmonics, the response decreased to a low near 20 Hz, and then increased to a peak near 140 Hz, before falling off at higher frequencies. A similar response was measured in monkey "R" (figure 2.3B).

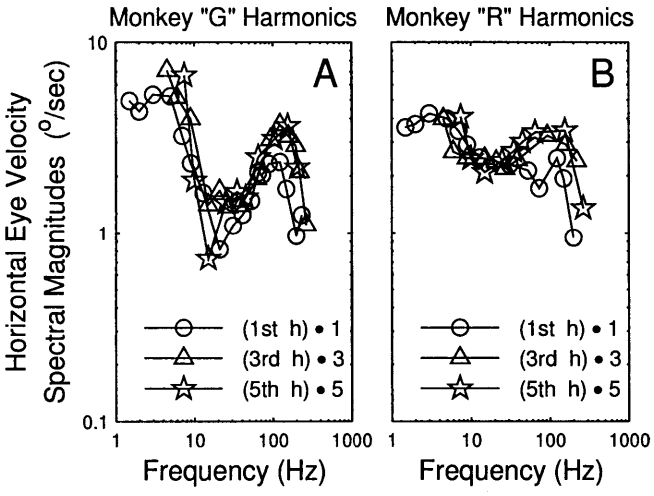

Figure 2.3. Horizontal eye velocity spectrum magnitudes at the first (o), third (Δ), and fifth (★) harmonics. Panel (A) shows results for monkey "G" and panel (B) shows results for monkey "R". Responses at the fundamental frequency (o) were used to sweep out a frequency response. Square wave modulated stimulation has components at odd harmonics of the fundamental frequency, and the strength of these components varies inversely with frequency. Therefore, responses at the third harmonics were scaled up by a factor of 3. Similarly, responses at the fifth harmonics were scaled up by a factor of 5. For these harmonics, points were plotted if they had a peak clearly above the noise floor. The frequency magnitude responses of the higher harmonics was similar to the response of the fundamental, consistent with linear system dynamics.

Beyond the 5th harmonic, a similar consistent pattern was also seen in all higher harmonics that had a clear spectral peak above the surrounding noise floor. Since responses from these harmonics are consistent with each other, this is consistent with linearity and time-invariance in the dynamics of the central VOR as tested here.

Based on the consistency of responses at higher harmonics, frequency response graphs were created by combining spectral response data from experiments at different modulation frequencies. Figure 2.4A shows the magnitude response for monkey "G". It is fairly flat from 1.5 to 5 Hz, decreases to a low near 20 Hz, and then increases to a peak near 140 Hz, before falling off at higher frequencies. The magnitude response from 1.5 to 150 Hz is constant within an order of magnitude, compared to a first order filter response which would fall off by two orders of magnitude over the same frequency range.

Starting with the fundamental, successive odd harmonics of each modulation frequency were included if they had a clear peak above the surrounding noise floor, judged by eye. The additional points from higher harmonics give a much fuller graph and substantially clarify the patterns in the results.

The unwrapped phase[3] response for monkey "G" is shown in figure 2.4B. The phase has a lead below 5 Hz. At higher frequencies the phase lags; the lag clearly increases with frequency, consistent with the effect of pure delay[4] in the simple VOR.

Figures 2.4C and 2.4D show the responses for monkey "R". As with monkey "G", the magnitude response is fairly flat from 1.5 to 5 Hz, decreases to a low near 20 Hz, and then increases to a peak near 140 Hz, before falling off at higher frequencies. The phase is also similar to the response in monkey "G".

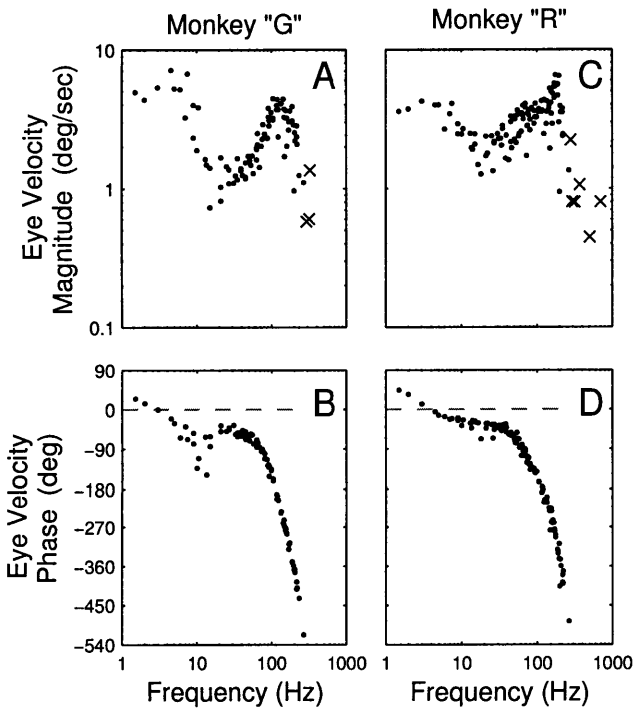

Figure 2.4. Frequency responses using 5000 pps. (A) and (C) show horizontal eye velocity magnitude responses for monkeys "G" and "R" respectively. These plots show all consecutive harmonics for which there was a peak clearly above the noise floor. As in figure 2.3, these peak magnitudes were multiplied by the harmonic number, to make them comparable to one another. The magnitude responses are fairly flat up to 10 Hz, decline to a low near 20 Hz, and then rise to a peak near 140 Hz, before falling off sharply at higher frequencies. The (x) markers show frequencies at which artifacts became more influential. They are plotted in the magnitude responses to provide an upper bound; the actual magnitude response is below the (x) marks at those frequencies. (B) and (D) show corresponding unwrapped phase responses. In both phase responses, the predominant feature is the increase in phase lag as a function of frequency, consistent with the effect of pure delay in the simple VOR. Below 5 Hz there is a phase lead (the dashed gray line shows a phase of 0°).

[3] The unwrapped phase is the phase, adjusted to eliminate discontinuities of 360 degrees or more

[4] A pure delay is a simple time delay, i.e. a delay of T has Laplace transform $\exp(-sT)$

VOR Frequency Response Tests with 250 pps

The frequency responses from 250 pps stimulation are shown in figure 2.5. Figure 2.5A shows relative magnitude responses. For all data sets, responses are constant within about an order of magnitude, and increase between 20 Hz and 100 Hz. For each data set, the magnitude response has been scaled to make the mean equal to 1, to facilitate comparison of results from different electrode preparations. As with experiments using 5000 pps, data points consist of all consecutive odd harmonics – from each modulation frequency – that had a clear peak above the surrounding noise floor.

The phases (figure 2.5B) follow similar delay curves. For monkey "N", phase data from left ear stimulation was shifted by 180° to make it comparable with data from right ear stimulation.

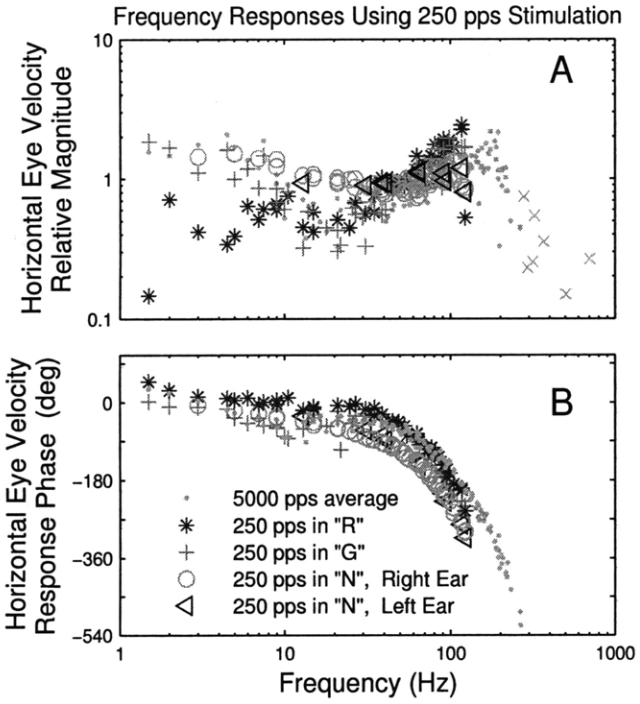

Figure 2.5. Frequency responses using 250 pps. (A) Relative magnitude responses of horizontal eye velocity are constant within about an order of magnitude, and increase between 20 Hz and 100 Hz. Responses have been scaled to make the mean equal to 1 for each data set, to facilitate comparison of results from different electrode preparations. As in figure 2.4, data points consist of all consecutive odd harmonics from each modulation frequency that had a clear peak above the surrounding noise floor. (B) Phase responses follow similar delay curves. For monkey "N", phase data from left ear stimulation was shifted by 180° to make it comparable with data from right ear stimulation.

Model of Frequency Response

The frequency response was modeled using extant linear system models of VOR central processing and the oculomotor plant. The block diagram is shown in figure 2.6.

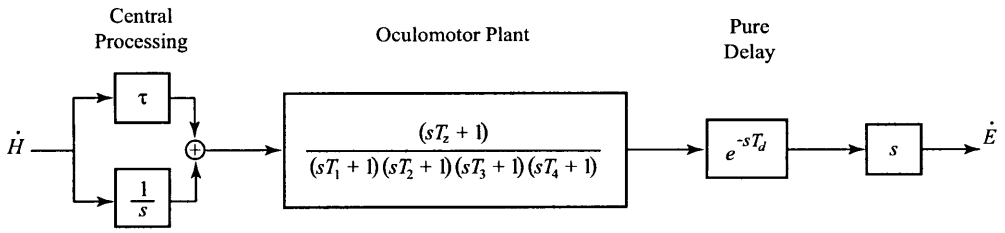

Figure 2.6. Model of central processing and oculomotor plant (where s is the Laplace variable). The head angular velocity, $\dot{H}$, is either sensed by the vestibular system or provided by the prosthesis. Central processing includes a direct and an integrated path. If the gain in the direct path is set to $\tau = T_1$ then central processing cancels the pole in the plant with the dominant time constant. The plant model is based on Robinson's model of the human eye, with parameters modified for the size of the squirrel monkey eye (see text for parameter values). The low-pass nature of the plant corresponds to the high order denominator. The pure delay term, $\exp(-sT_d)$, models the delays due to synaptic neurotransmitter release and neural conduction. To easily compare the output to the input velocity $\dot{H}$, a differentiator ("s") and the eye velocity, $\dot{E}$, are represented schematically.

For the oculomotor plant, we used Robinson's 4th order linear model (Robinson 1964) with the following transfer function:

$$\frac{\theta(s)}{\Delta R(s)} = \frac{sT_z + 1}{(sT_1 + 1)(sT_2 + 1)(sT_3 + 1)(sT_4 + 1)} \tag{1}$$

where s is the Laplace variable, ΔR is the fluctuation of the oculomotor firing rate above or below its baseline rate, and θ is the eye position.

The model for central processing is inferred from knowledge of the vestibular signals, the oculomotor plant, and the overall VOR response (Robinson 1981). The vestibular signals consist of velocity signals, whereas the ocular motoneuron firing rates are functions of both velocity and position terms (Robinson 1970), implying that in addition to the direct path, a parallel neural integrator is part of central processing. The integration for horizontal motion is thought to occur in many structures including the medial vestibular nucleus and the nucleus prepositus hypoglossi (Kaneko 2006, Fukushima and Kaneko 1995). Thus, central processing is modeled by the transfer function $\tau + (1/s)$. Also, the overall empirical VOR transfer function does not include the long time constant T_1 of the oculomotor plant, i.e. that pole appears to be cancelled by central processing (Skavenski and Robinson 1973, Robinson 1981). This would occur if the gain of the direct path were $\tau = T_1$, which is what we used. Then the central processing transfer function becomes $T_1 + (1/s) = (T_1 s + 1)/s$, which has a system zero that cancels the dominant pole of the oculomotor plant.

In the model of central processing, the effect of the direct path is predominant compared to the effect of the integrated path. The value of τ that we used in the central processing network corresponds to a break frequency of 0.57 Hz, which is lower than the 1.5–701 Hz frequency range that we used in experiments. In this frequency range the neural integrator plays a minor role, since the neural integrator's magnitude response scales inversely with frequency. We should also consider that the neural integrator has

not been explicitly tested in this frequency range, and we should be cautious in assuming that it continues to work in this range. Moreover, the neural integrator may not be working in our experiments, due to the nature of our unilateral stimulation. We provided the stimulated ear with a baseline rate that was above the contralateral ear's spontaneous rate, in order to ensure there were many pulses per modulation cycle. However, it is worth bearing in mind that neural network models suggest that the neural integrator relies on lateral inhibition (Cannon et al 1983; Arnold and Robinson 1997) to function. In all these cases, the direct path plays the predominant role in the central processing network.

Our model consists of the central processing network followed by the oculomotor plant, as well as the pure delay term, $\exp(-sT_d)$, which models the delays due to synaptic neurotransmitter release and neural conduction (Robinson 1981, Minor et al. 1999). We did not include the dynamics of the peripheral vestibular afferents, because our electrical stimulation bypasses the canals and stimulates the vestibular nerve directly. We did not include velocity storage, which involves filtering by the vestibular nuclei to prolong the peripheral time constant (Robinson 1977), because it would only make a significant difference below about 0.1 Hz, which is far below our lowest stimulation frequency.

Figure 2.7 shows frequency response data along with model response curves. For data sets, the magnitude responses have been scaled to make the mean equal to 1, to facilitate comparison of results from different electrode preparations. The frequency responses obtained using 5000 pps were then averaged, using a Cartesian average incorporating magnitude and phase. Responses using 250 pps were similarly scaled and averaged.

The dashed blue curves show the response of the model using parameter values from the literature. Robinson characterized the oculomotor plant for human subjects, but the model parameters have been adjusted for rhesus monkeys (Fuchs et al. 1988) and squirrel monkeys (Minor et al. 1999), which we used. Because we used only an eye coil rather than a contact lens as Robinson did, we estimate that the moment of inertia of the eye coil (0.00504×10^{-4} g·sec^2/deg) was negligible compared to that of the eye (Minor and colleagues used 0.0732×10^{-4} g·sec^2/deg). We used the following parameter values: T_z=0.14, τ=T_1=0.28, T_2=0.037, T_3=0.003, and T_4=0.0004 seconds. We then used T_d=0.004 seconds to fit the phase response. The model response fits the data within a factor of about 3 at both low and high frequencies. However, the model does not fit the detailed shape of the data, perhaps because the model parameters were estimated using data at much lower frequencies than in the present data set.

The solid red curve in figure 2.7 shows the fit when the same model has its parameters manually adjusted to match the data. Motivated by the fact that the data seems to exhibit a resonance near 140 Hz, the model was adjusted and two poles were combined into a resonant pair, with a peak near 140 Hz. This is qualitatively similar to the fact that both Robinson (Robinson 1968) and Thomas (Thomas 1967) used a resonant pair for the upper two poles in their models of the human eye plant. The exact parameters we used were: τ=0.80, T_z=0.018, T_1=0.16, and T_2=0.037 seconds, and the complex conjugate poles had imaginary parts at ±150 Hz and real parts at -45 Hz[5]. A value of T_d=0.004 seconds again made a good fit to the phase response. For both the model with literature parameters and the model with adjusted parameters, the plant's high order denominator, cuts off responses above 150 Hz.

[5] In other words, the peak magnitude response for this pole pair occurred at 143 Hz, the damping ratio was ξ=0.287, and the undamped natural frequency was f_n=157 Hz

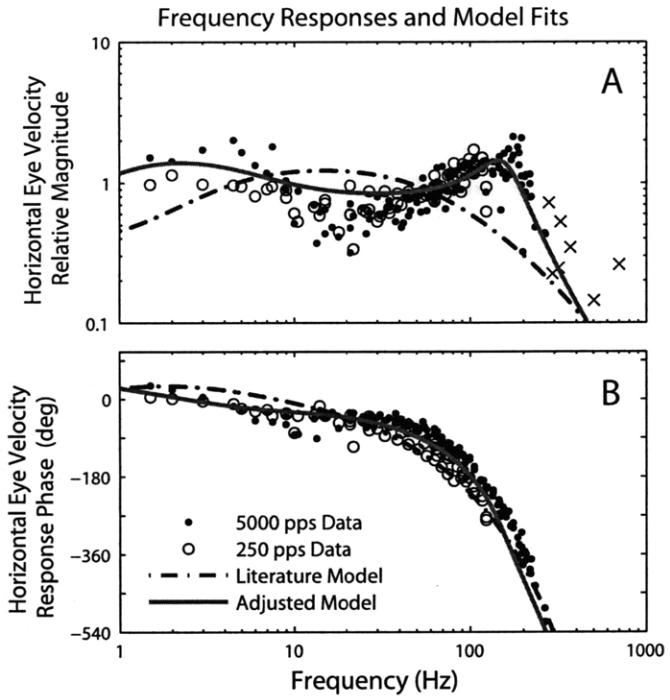

Figure 2.7. Model fits. From experiments using 5000 pps, data from monkeys "G" and "R" were scaled and averaged (•). The (x) markers show frequencies at which artifacts became more influential. They are plotted in the magnitude response to provide an upper bound; the actual magnitude response is below the (x) marks at those frequencies. From experiments using 250 pps, data from monkeys "G", "R", "N" right ear, and "N" left ear were scaled and averaged (o). The dashed blue curves show the response of the model using parameter values from the literature, which has all real poles for the squirrel monkey. For the solid red curves, the two highest frequency poles have been combined into a resonant pair with a maximum magnitude response at 143 Hz (see text for all parameter values).

CONTROL TESTS AND ARTIFACTS

Control tests verified that eye movements at most of the high frequencies reported here were physiological, not artifactual. During control tests, the monkey was tested before and after administration of anesthesia. Figure 2.8A confirms that before anesthesia, the eye movement spectrum at 3 Hz, and at odd harmonics, was similar to the spectrum in figure 2.1C. Both tests used stimulation with 5000 pps and 3 Hz modulation. In figure 2.8A, no d-amphetamine was used, but the monkey remained awake for this short test, and eye movements at 3 Hz were clearly visible on a monitor displaying the image from an infrared camera.

When the monkey was deep under pentobarbital anesthesia (> 30 minutes after injection), variations in the eye signal were tiny when electrical stimulation was applied to the canal electrode (figure 2.8B). Figure 2.8C tracks the time evolution of the 3 Hz component before and after anesthesia. This eye movement component reduced 100-fold when the squirrel monkey was under anesthesia.

A similar trend occurred when the modulation frequency was 267 Hz. When the monkey was awake (figure 2.8D), there was a clear eye movement component at 267 Hz, which was abolished by anesthesia (figure 2.8E). When tracked before and after anesthesia (figure 2.8F), this component showed a 5-fold reduction under anesthesia.

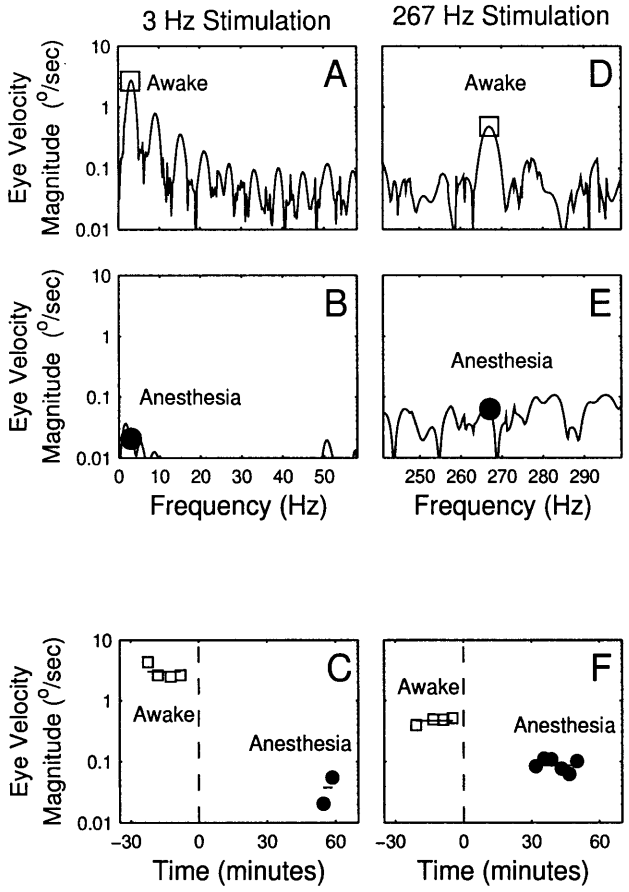

Figure 2.8. Control tests verified low levels of artifacts at two frequencies in monkey "G". When stimulation had 3 Hz modulation and the animal was awake (A), its horizontal eye movement magnitude spectrum had a large peak at 3 Hz (□). However when the monkey was under anesthesia (B), the response at 3 Hz was much smaller (•). (C) shows that when tested many times, these responses were consistent (the solid horizontal lines show averages). Similarly for 267 Hz stimulation, (D) shows a large response when the animal was awake, (E) shows a much smaller response under anesthesia, and (F) shows consistency when tested many times. In (C) and (F), the dashed vertical lines show the time when anesthesia was administered. All measurements under anesthesia were taken at least half an hour after anesthesia was administered, while the animal was deep under anesthesia.

Anesthesia tests were done at many frequencies, and the ratios of the awake to anesthesia magnitude responses are plotted in figure 2.9. The awake response was very much larger than the anesthesia response (more than 250%) up to 267 Hz. At 293 Hz the awake response was still significantly larger (more than 75%) than the anesthesia response. However at 317, 503, and 701 Hz, the anesthesia response was at least as large as the awake response, indicating significant artifacts.

Similar results were obtained in a euthanasia test. Monkey "G" was tested while awake without d-amphetamine, and then after euthanasia. While the monkey was awake, the responses at 89 and 267 Hz were very much greater than they were shortly after euthanasia, as well as several hours afterwards, when rigor mortis was setting in. However, the response at 701 Hz was similar before and after euthanasia, again indicating significant artifacts at that high frequency.

Therefore we could not attribute the eye coil signal spectral peaks at 317, 503, and 701 Hz to physiologic responses. Responses at frequencies above 267 Hz are not included in any other plots here, except as indicated by the (x) symbol in figures 2.4 and 2.6, to show an upper bound for the magnitude responses.

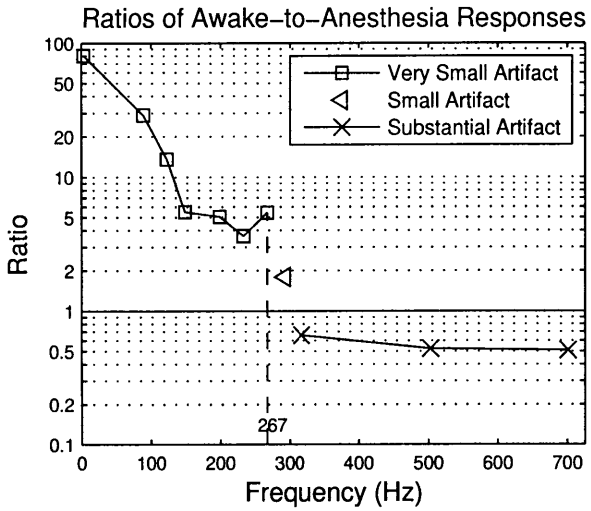

Figure 2.9. Artifacts dominate response at higher frequencies. Anesthesia responses were shown in figure 2.8 for two frequencies. Here the ratios of awake-to-anesthesia responses of horizontal eye velocity are shown at many frequencies. Awake responses were very much larger than (more than 250% larger than) the anesthesia responses for stimulation at 267 Hz and below (□), indicating that artifacts were very small. At 293 Hz (◁) the awake response was still significantly larger (more than 75% larger), but at higher frequencies (x) the anesthesia response was as large or larger, indicating the presence of significant artifacts.

Discussion

Using peripheral electrical stimulation, we have measured the angular VOR in the squirrel monkey at much higher frequencies than are practical to apply by physically rotating subjects. We have shown that the VOR response is found well above 50 Hz, and extends above 200 Hz, even though the oculomotor plant is strongly low-pass. The VOR phase response showed a clear lag with frequency, consistent with the effect of pure delay in the simple VOR.

It is important to note that our results are frequency responses from extracellular electrical stimulation using pulses of a constant current amplitude. When physical rotation is used, stimulation at different velocities recruits different afferents with different thresholds and dynamics, whereas our electrical stimulation probably recruits the same population of afferents for all modulation frequencies. The frequency responses shown here are the magnitude and phase responses to electrical stimulation.

MAGNITUDE RESPONSE OF VOR

The VOR magnitude response was constant within an order of magnitude from 1.5 to 250 Hz (figures 2.4A and 2.4C), compared to a first order filter response which would fall off by more than two orders of magnitude over the same frequency range. From 1.5 to 5 Hz, the magnitude response was fairly flat. Similar results have been obtained when physical rotation has been used over the same frequency range.

The magnitude response in our study decreased from 5 to 20 Hz, and then increased to a peak just above 100 Hz. These trends might be due to the latency, magnitude, and phase properties of the unmodifiable and modifiable pathways of the VOR (Ramachandran and Lisberger 2006). The neural network that brings the head velocity signal from the vestibular periphery to the oculomotor plant consists of two pathways, a direct path (the simple VOR), and a parallel path that goes through the cerebellum and is capable of learning. The latter pathway has a latency 7.5 ms longer than the former,

and the gain and phase of these pathways have been characterized from 0.5 to 50 Hz (Ramachandran and Lisberger 2006). Based on these characteristics, our magnitude response decrease from 5 to 20 Hz may be due to destructive interference as the two VOR pathways become out of phase with each other, and our magnitude response increase between 20 and 100 Hz may be due to constructive interference as their phases align. Physical rotation studies have also found an increasing magnitude response from 25 to 50 Hz (Ramachandran and Lisberger 2005). In our study, this increase continued up to 140 Hz.

Physical rotation studies in the rhesus monkey have not found a decrease from 5 to 20 Hz as we did, but perhaps this is because the species have slightly different transfer functions for the simple and the learning pathways. On the other hand, physical rotation studies in the squirrel monkey (Minor et al. 1999) have found a flat VOR magnitude response from 5 to 15 Hz. We do not know why we obtained a different response in this frequency range.

Phase Response of VOR

The phase response showed a clear lag with frequency (figures 2.4B and 2.4D). We attribute this to two effects: (1) mainly to the effect of a 4 ms pure delay in the three-neuron arc of the simple VOR, and (2) partially to a 180 degree phase lag coming from the transfer function of the model of the oculomotor plant and central processing. A similar delay for the VOR was also measured in another study (Merfeld et al. 2007).

When physical rotation has been used to study the VOR, a similar phase lag has been found from 25 to 50 Hz (Ramachandran and Lisberger 2005). However, in the range from 10 to 25 Hz, studies using physical rotation have not found significant phase lag (Minor et al. 1999; Huterer and Cullen 2002; Ramachandran and Lisberger 2005). The lag effect of the VOR delay may be cancelled by the phase lead of the canal afferents (Fernandez and Goldberg 1971). Those dynamics are included when physical rotation is used, whereas they are bypassed by our electrical stimulation. Finally, in the range from 1.5 to 10 Hz, there is little phase lag in either our study or in studies using physical rotation. The VOR latency corresponds to a small phase lag in this frequency range.

Control Tests and Artifacts

Control tests were important to rule out artifacts because the ear was stimulated electrically, and the eye coil was just centimeters away. Both inductive and capacitive artifacts increase linearly with frequency, and we probed the VOR at much higher frequencies than have been previously reported. To verify that the eye coil signals we measured were physiological eye movements, rather than artifacts caused by the small current from the electrodes passing through the tissue, we conducted control tests using general anesthesia and euthanasia. Artifacts were much smaller than the physiological response at 267 Hz and below. However, at 317 Hz and above, artifacts were significant compared to the physiological response.

The firing rate of the peripheral vestibular nerve can be as high as 400 spikes/s, abducens internuclear neurons have firing rates up to 800 spikes/s (Fuchs et al. 1988), and the ocular motoneurons have firing rates up to 400 spikes/s (Goldberg and Fernandez 1971, Fuchs et al. 1988). This raises the question whether the nervous system can transmit information at 400 Hz, or even higher frequencies if parallel pathways were stimulated asynchronously. For example, regular units are thought to accept inputs from a large number of sources, and therefore be continuously charging up steadily, so in a pool of regular units there are always some neurons very near threshold

and ready to fire upon being stimulated. We used stimulation at 5000 pps, well above the maximum peripheral firing rate, and tried modulation frequencies up to 701 Hz. Spectral peaks were indeed measured up to 701 Hz in the eye coil signal. However, since we determined that our responses at 317 Hz and above have significant artifacts, our data can't be used to address this question of asynchronous responses.

CONCLUSIONS

Using peripheral electrical stimulation, we have shown that the frequency response of central angular VOR pathways in the squirrel monkey extends well above the ranges previously explored using physical rotation (15 Hz in the squirrel monkey and 50 Hz in the rhesus monkey). We do not believe the response has an ecologic function at such high frequencies. Nevertheless, this work shows that the nervous system is capable of transmitting modulated signals up to at least 267 Hz, supporting the viability of vestibular prostheses that use stimulation modulated around a baseline rate that is substantially higher than the spontaneous rate. This work also demonstrates that eye movements can be evoked up to 267 Hz, even though the oculomotor plant has strongly low-pass characteristics.

Similar to studies using physical rotation, from 20 to 50 Hz the magnitude response had a slight increase, and the phase had a substantial lag from 25 to 50 Hz. In the magnitude response, the roll-off above 150 Hz is consistent with the strongly low-pass character of the oculomotor plant, which is modeled by a transfer function with four poles and only a single zero. In the phase response, the phase lag is consistent with the effect of pure delay in the three-neuron arc of the simple VOR.

Acknowledgements

We thank Richard Lewis for eye coil surgeries, Jennifer Morrissey for assistance with the animals, and Margaret Lankow for administrative support. We appreciate the helpful comments from M. Saginaw's thesis committee: Charles Oman, Louis Braida, Richard Lewis, and Steve Massaquoi. This paper is a portion of a doctoral thesis (Saginaw 2010) submitted to the Department of Electrical Engineering and Computer Science, Massachusetts Institute of Technology, Cambridge MA, in partial fulfillment of requirements for the degree of Doctor of Philosophy.

Grants

Support from NIH F31 DC006202, R01 DC03066, and R01 DC008167, and European Commission 225929 gratefully acknowledged.

References

Arnold DB, Robinson DA. The oculomotor integrator: testing of a neural network model. *Exp Brain Res* 113: 57-74, 1997.

Babb TL, Soper HV, Lieb JP, Brown WJ, Ottino CA, Crandall PH. Electrophysiological studies of long-term electrical stimulation of the cerebellum in monkeys. *J Neurosurg* 47: 353-365, 1977.

Cannon SC, Robinson DA, Shamma S. A proposed neural network for the integrator of the oculomotor system. *Biol Cybern* 49: 127-136, 1983.

Della Santina CC, Migliaccio AA, Patel AH. A multichannel semicircular canal neural prosthesis using electrical stimulation to restore 3-D vestibular sensation. *IEEE Trans Biomed Eng* 54, 1016-1030, 2007.

Fernandez C, Goldberg JM. Physiology of peripheral neurons innervating semicircular canals of the squirrel monkey. II. Response to sinusoidal stimulation and dynamics of peripheral vestibular stimulation. J Neurophysiol 34: 661-675, 1971.

Fuchs AF, Scudder CA, Kaneko CRS. Discharge patterns and recruitment order of identified motoneurons and internuclear neurons in the monkey abducens nucleus. *J Neurophysiol* 60: 1874-1895, 1988.

Fukushima K, Kaneko CRS. Vestibular integrators in the oculomotor system. *Neurosci Res* 22: 249-258, 1995.

Gauthier GM, Piron JP, Roll JP, Marchetti E, Martin B. High-frequency vestibulo-ocular reflex activation through forced head rotation in man. *Aviat Space Environ Med* 55: 1-7, 1984.

Goldberg JM, Fernandez C. Physiology of peripheral neurons innervating semicircular canals of the squirrel monkey. I. Resting discharge and response to constant angular accelerations. J Neurophysiol 34: 635-660, 1971.

Gong W, Merfeld DM. Prototype neural semicircular canal prosthesis using patterned electrical stimulation. *Ann Biomed Eng* 28: 572-581, 2000.

Gong W, Merfeld DM. System design and performance of a unilateral horizontal semicircular canal prosthesis. *IEEE Trans Biomed Eng* 49, 175-181, 2002.

Gong W, Haburcakova C, Merfeld DM. Vestibulo-ocular responses evoked via bilateral electrical stimulation of the lateral semicircular canals. *IEEE Trans Biomed Eng* 55: 2608-2619, 2008.

Huterer M, Cullen KE. Vestibuloocular reflex dynamics during high-frequency and high-acceleration rotations of the head on body in rhesus monkey. *J Neurophysiol* 88: 13-28, 2002.

Judge SJ, Richmond BJ, Chu FC. Implantation of magnetic search coils for measurement of eye position: an improved method. *Vision Res* 20: 535-538, 1980.

Kaneko CRS. Effects of ibotenic acid lesions of nucleus prepositus hypoglossi on optokinetic and vestibular eye movements in the alert, trained monkey. *Ann NY Acad Sci* 656: 408-427, 2006.

Lasker DM, Backous DD, Lysakowski A, Davis GL, Minor LB. Horizontal vestibuloocular reflex evoked by high-acceleration rotations in the squirrel monkey. II. Responses after canal plugging. *J Neurophysiol* 82: 1271-1285, 1999.

Lewis RF, Gong W, Ramsey M, Minor L, Boyle R, Merfeld DM. Vestibular adaptation studied with a prosthetic semicircular canal. *J Vestib Res* 12: 87-94, 2002/2003.

Merfeld DM, Gong W, Morrissey J, Saginaw M, Haburcakova C, Lewis RF. Acclimation to chronic constant-rate peripheral stimulation provided by a vestibular prosthesis. *IEEE Trans Biomed Eng* 53: 2362-2372, 2006.

Merfeld DM, Haburcakova C, Gong W, Lewis RF. Chronic vestibulo-ocular reflexes evoked by a vestibular prosthesis. *IEEE Trans Biomed Eng* 54: 1005-1015, 2007.

Minor LB, Lasker DM, Backous DD, Hullar TH. Horizontal vestibuloocular reflex evoked by high-acceleration rotations in the squirrel monkey. I. Normal responses. *J Neurophysiol* 82: 1254-1270, 1999.

Mortimer JT. Electrical excitation of nerve. In: *Neural Prostheses: Fundamental Studies*, edited by Agnew, WF and McCreery DB. Englewood Cliffs, NJ: Prentice Hall, 1990, p. 67-83.

Oppenheim AV, Schafer RW, Buck JR. Periodogram Averaging. In: *Discrete-Time Signal Processing, Second Edition*. Upper Saddle River, New Jersey: Prentice Hall, 1999, sect. 10.6.3, chapt. 10, Fourier analysis of signals using the discrete Fourier transform, p. 737-738.

Paige G. Vestibuloocular reflex and its interactions with visual following mechanisms in the squirrel monkey. I. Response characteristics in normal animals. *J Neurophysiol* 49: 134-151, 1983.

Paige G. Vestibuloocular reflex and its interactions with visual following mechanisms in the squirrel monkey. II. Response characteristics and plasticity following unilateral inactivation of horizontal canal. *J Neurophysiol* 49: 152-168, 1983.

Ramachandran R, Lisberger SG. Normal performance and expression of learning in the vestibulo-ocular reflex (VOR) at high frequencies. *J Neurophysiol* 93: 2028-2038, 2005.

Ramachandran R, Lisberger SG. Transformation of Vestibular Signals Into Motor Commands in the Vestibuloocular Reflex Pathways of Monkeys. *J Neurophysiol* 96: 1061-1074, 2006.

Robblee LS, Rose TL. Electrochemical guidelines for selection of protocols and electrode materials for neural stimulation. In: *Neural Prostheses Fundamental Studies*, edited by Agnew WF and McCreery DB. Englewood Cliffs, NJ: Prentice Hall, 1990, p. 25-66.

Robinson DA. A method of measuring eye movement using a scleral search coil in a magnetic field. *IEEE Trans Biomed Eng* 10: 137-145, 1963.

Robinson DA. The mechanics of human saccadic eye movement. *J Physiol* 174: 245-264, 1964.

Robinson DA. The oculomotor control system: A review. *Proc IEEE* 56: 1032-1049, 1968.

Robinson DA. Oculomotor unit behavior in the monkey. *J Neurophysiol* 33: 393-404, 1970.

Robinson DA. Vestibular and optokinetic symbiosis: an example of explaining by modeling. In: Control of gaze by brain stem neurons, developments in neuroscience, Vol. 1, edited by Baker R, Berthoz A. Amsterdam: Elsevier/North-Holland Biomedical Press, 1977.

Robinson DA. The use of control systems analysis in the neurophysiology of eye movements. *Ann Rev Neurosci* 4: 463-503, 1981.

Saginaw MA. *Eye Movement Studies with a Vestibular Prosthesis* (Ph.D. Thesis). Cambridge MA: Massachusetts Institute of Technology, 2010.

Saginaw MA, Gong W, Haburcakova C, Merfeld DM. Angular vestibulo-ocular reflex above 100 Hz elicited by electrical stimulation of the vestibular peripheral nerve. II. Responses in the guinea pig. *J Neurophysiol to be submitted 2009*.

Shepherd RK, Franz BK-H, Clark GM. The biocompatibility and safety of cochlear prostheses. In: *Cochlear Prostheses*, edited by Clark GM, Tong YT, and Patrick JF. Edinburgh: Churchill Livingstone, 69-98, 1990.

Skavenski AA, Robinson DA. Role of abducens neurons in vestibuloocular reflex. J Neurophysiol 36: 724-738, 1973.

Thomas JG. The torque-angle transfer function of the human eye. *Kybernetik* 3: 254-263, 1967.

Vercher JL, Gauthier GM, Marchetti E, Mandelbrojt P, Ebihara Y. Origin of eye movements induced by high frequency rotation of the head. *Aviat Space Environ Med* 55: 1046-1050, 1984.

Chapter 3

Angular Vestibulo-Ocular Reflex Above 100 Hz Elicited by Electrical Stimulation of the Vestibular Peripheral Nerve. II. Responses in the Guinea Pig

Saginaw, Michael A.[1,2]
Gong, Wangsong[2,3]
Haburcakova, Csilla[2,3]
Merfeld, Daniel M.[2,3]

1. Department of Electrical Engineering and Computer Science, Massachusetts Institute of Technology, Cambridge MA

2. Jenks Vestibular Physiology Laboratory, Massachusetts Eye and Ear Infirmary, Boston MA

3. Department of Otology and Laryngology, Harvard Medical School, Boston MA

Abstract

The angular vestibulo-ocular reflex (VOR), which stabilizes gaze during head motion, has previously been characterized up to 2 Hz in guinea pigs and 50 Hz in monkeys by physically rotating subjects. To study the VOR neural network at higher frequencies, we electrically stimulated the peripheral vestibular nerve in awake guinea pigs. Stimulation consisted of biphasic charge-balanced pulses that were gated on or off by square wave modulation. The modulation frequency was varied from 1.5 to 293 Hz to obtain the frequency response. Spectral responses were computed using the fast Fourier transform. The VOR magnitude response was constant within an order of magnitude from 1.5 to 151 Hz. It was fairly flat up to 8 Hz, increased to a peak near 50 Hz, and decreased at higher frequencies, in agreement with the high frequency fall-off expected from Robinson's fourth order mechanical model of the eye. The phase response had a clear lag as a function of frequency, consistent with a 4 ms pure delay in the simple VOR. We concluded that the nervous system is capable of conveying modulated signals above 100 Hz, and that eye movements can be measured at these frequencies, even though the oculomotor plant has strongly low-pass characteristics. Both the magnitude and phase responses were consistent with signals at these high frequencies being transmitted by the simple VOR three-neuron arc.

Introduction

The vestibular system senses head motion and generates compensatory eye movements in order to help stabilize gaze. This response is known as the vestibulo-ocular reflex (VOR). In particular, angular head motion is sensed by the semicircular canals, which evoke the angular VOR. Previous studies have characterized the angular VOR up to 2 Hz in guinea pigs (Escudero et al. 1993; Andrews et al. 1997; Pettorossi et al. 1986). The VOR has also been characterized up to 15 Hz in squirrel monkeys and 50 Hz in rhesus monkeys (Paige 1983; Huterer and Cullen 2002; Minor et al. 1999; Ramachandran and Lisberger 2005). Those studies showed that the gain is near 1 up to 20 Hz, and increases towards 3 at higher frequencies. The phase is compensatory for head motion up to 25 Hz, and lags head motion at higher frequencies.

Here we describe an investigation of the angular VOR at higher frequencies in the guinea pig, using electrical stimulation. A companion paper (Saginaw et al. 2009) describes a similar investigation in the squirrel monkey. It is interesting to study the VOR at higher frequencies to explore whether the reflex functions up to the maximum firing rate of peripheral neurons or even higher, to study the VOR above 25 Hz where the reflex does not show adaptation (Ramachandran and Lisberger 2005), and to characterize the reflex at frequencies used by neuro-vestibular prostheses (Gong and Merfeld 2000, 2002; Della Santina et al. 2007). The first generation of these prostheses have been mostly unilateral, and in order to provide bidirectional motion cues above the spontaneous rate, the prostheses use high baseline rates such as 200 pulses per second (pps). Since the modulated output often extends above 300 pps, it is important to characterize the VOR up to these frequencies.

It is very difficult to provide stimulation above 50 Hz with carefully controlled spectral content using physical motion devices, but feasible to do so using electrical stimulation. As part of a project to develop a vestibular implant, analogous to cochlear implants for the deaf, we used electrical stimulation to elicit eye movements at much higher frequencies than previously studied, and characterized the response of the angular VOR from 1.5 to 293 Hz. Since the oculomotor plant is strongly low-pass, and guinea pig eye movements are slower than those in monkeys or humans, we hypothesized that the VOR magnitude response would fall off above 25 Hz in guinea pigs. We hypothesized that the phase response would lag linear with frequency, due to the latency of the three-neuron arc of the simple VOR.

Methods

Surgeries, instrumentation, experiments and data analysis were similar to procedures described in the companion paper on the squirrel monkey (Saginaw et al. 2009), so only brief descriptions are provided here.

Animal Preparation

Four mature (> 700 g), male, pigmented guinea pigs (*Cavia porcellus*), designated as "S", "D", "G", and "O", were used as subjects. All work with animals adhered to a protocol approved by the Institutional Animal Care and Use Committee of the Massachusetts Eye and Ear Infirmary. During all surgeries, animals were under Isoflurane general anesthesia, and sterile instruments and materials were used.

A head bolt made of a composite ("G10") was attached to the skull, and was used to secure in place a head cap that housed electronics on top of the head. An eye coil 11

mm in diameter, made of three turns of stainless steel wire, was implanted on one eye to measure eye position. An incision was made in the right ear and an electrode was implanted in the ampulla of the lateral semicircular canal, to stimulate the vestibular nerve. In order to ensure that the electrode was positioned in the ampulla of the lateral canal, we briefly provided electrical stimulation during surgery to verify that eye movements were predominantly horizontal, and adjusted the electrode position using a micromanipulator as necessary. The lateral canal was also plugged to prevent modulation of the vestibular nerve signal by yaw rotation. Following surgeries, animals were allowed to rest at least 14 days before testing.

VOR Frequency Response Tests

During experiments the guinea pigs were held stationary on a custom fabricated test platform. The platform held the head cap, and fixed the head position at a forward pitch angle of approximately 45°, in order to bring the lateral canals approximately parallel with earth-horizontal. The platform also positioned the animal so that its eyes were in the center of the frame of the search coil system. Experiments were conducted in the dark, in order to focus on vestibular-driven eye movements.

Electrical stimulation was delivered to the electrode implanted in the ampulla of the lateral canal. The stimulation pattern is shown in figure 3.1A. Stimulation consisted of a pattern of charge-balanced biphasic pulses, shown at the top of figure 3.1A. Each biphasic pulse was composed of a negative (cathodic) current pulse lasting 50 μs, followed immediately by a positive (anodic) current pulse, also lasting 50 μs. For each animal, the current amplitude was chosen to be large enough to elicit eye movements, but small enough to not stimulate the facial nerve to cause facial twitching. Current amplitudes ranged from 100 to 200 μA across animals. These were below the charge delivery levels used in other experiments with long-term stimulation (Merfeld et al. 2006). All guinea pigs were tested with a biphasic pulse rate of 250 pps, which is well below the maximum neural firing rate of the peripheral vestibular nerve. In addition, animals "S", "D", and "G" were tested at 598 pps, which is well above the nerve's maximum firing rate.

As shown in the bottom of figure 3.1A, the biphasic pulse train was modulated by a square wave, which gated the pulse train on or off. Modulation frequencies were always less than half the biphasic pulse rate, in order to ensure that there was at least one pulse in each "on" portion of the modulation cycle. For biphasic pulses at 250 pps, the modulation frequencies ranged from 1.5 to 123 Hz. For biphasic pulses at 598 pps, the modulation frequencies ranged from 1.5 to 293 Hz. The modulation frequencies included 20 values from 1.5 to 293 Hz inclusive and were spaced approximately logarithmically. A few modulation frequencies were deliberately chosen as multiples of other modulation frequencies, e.g. 9 Hz was used in order to compare its results to those from the 3rd harmonic of 3 Hz, which was also a modulation frequency. However, most modulation frequencies were selected as prime numbers, to preclude possible interferences (e.g. 30 Hz was not chosen, to preclude possible confounding effects of the 60 Hz power system)[1].

Figure 3.1B shows the idealized neural stimulation in response to electrical stimulation. Within the "on" portion of the modulation, pulses are delivered to the vestibular nerve, and elicit action potentials.

[1] Modulation frequencies included 1.5, 2, 3, 5, 7, 9, 13, 21, 31, 41, 53, 65, 73, 89, 123, 149, 151, 199, 251, and 293 Hz

Figure 3.1C shows the spectrum of the pattern in figure 3.1B. The stimulation is formed by multiplying the biphasic pulse train by the modulating square wave. The square wave spectrum consists of components at the odd harmonics of the square wave's fundamental frequency, and the component magnitudes scale inversely with frequency. Since multiplication in the time domain corresponds to convolution in the frequency domain, the spectrum of the stimulation has the same pattern of components at odd harmonics of the square wave frequency, and the pattern is also replicated about the biphasic pulse frequency, as shown in the right part of figure 3.1C.

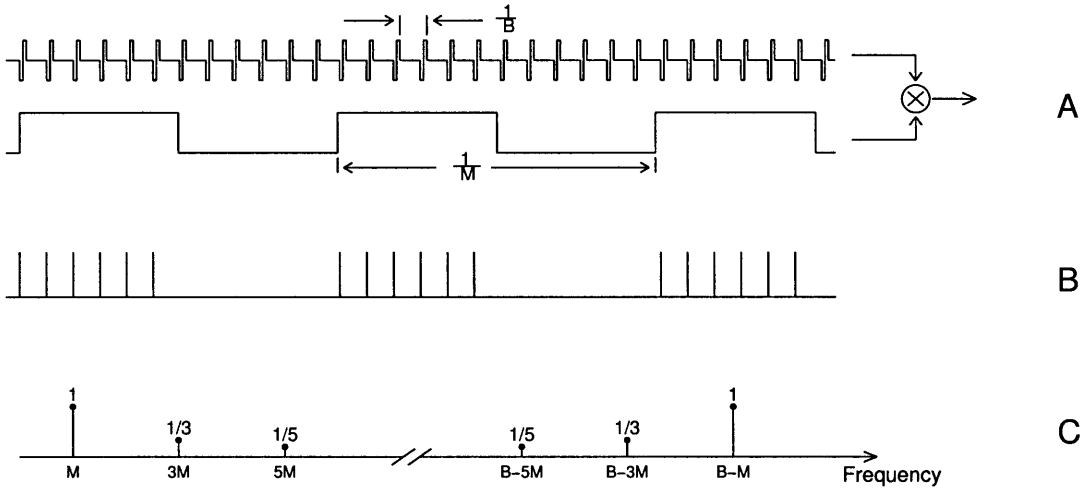

Figure 3.1. Stimulation paradigm. (A) In the time domain, the stimulation consists of a biphasic pulse train with *B* pulses per second, as shown at the top. This pulse train is multiplied by an on-or-off modulation square wave with a frequency of *M* Hz, as shown underneath. (B) In the idealized neural signal, each pulse that is in the "on" gate of the modulation elicits action potentials. Panel (C) shows the spectrum of the idealized neural signal. Since multiplication in the time domain corresponds to convolution in the frequency domain, the spectrum contains the odd harmonics in the square wave modulation, and the same pattern is replicated about the biphasic pulse rate B.

Stimulation duration was 10 seconds, but for modulation frequencies below 10 Hz the stimulation duration was 30 seconds in order to include enough data for analysis. These durations were kept short in order to prevent acclimation (Merfeld et al. 2006).

Eye position was measured using a Robinson (Robinson 1963) style search coil system (C-N-C Engineering, Seattle WA) with coil frequencies of 72 kHz and 108 kHz. The coil system's phase detector outputs were filtered for anti-aliasing by 5th order Bessel low pass filters with a -3dB frequency of 3000 Hz, and recorded at 12 kHz[2]. Sampling was done with a 16 bit analog-to-digital converter with a resolution of 320 μV

[2] The sampling rate was very close to 12 kHz. The data acquisition hardware was limited to integer multiples of its 50 ns clock, and we used the true sampling interval of 83.35 μs (~11.9976 kHz) in data analysis.

per bit (which corresponded to approximately 640 μdegrees/bit), on a data acquisition card controlled by LabView (both by National Instruments, Austin TX).

DATA ANALYSIS

Data processing and spectral analysis were carried out in MATLAB (The MathWorks, Natick MA). Eye movement spectra were computed using fast Fourier transforms of non-overlapping segments of eye position data. Segments were 1 second for modulation frequencies below 10 Hz, in order to include more than one cycle. For higher modulation frequencies, segments were ½ second in order to provide enough windows for averaging.

Portions of data with nystagmic quick phases and blinks were excluded from the analysis. Since quick phases are step-like signals, they were found to degrade the spectra by adding substantial low frequency noise. Typically the noise could affect the spectra up to 80 Hz in the guinea pig, and increased the spectral noise floor by a factor of 1.48. When quick phases and blinks were excluded, this reduced the number of usable data segments; data from a given modulation frequency was only used when there was a minimum of six usable data segments available for averaging.

Data segments were processed to remove the linear trend, to remove the slow phase of any spontaneous nystagmus the animal might have had in the dark. Data segments were then tapered by Hann windows to reduce spectral leakage, including leakage from all spectral peaks, and including peaks at power line harmonics. For the spectra, velocity was calculated in the frequency domain via multiplication by a frequency ramp. Spectra were scaled so that a magnitude of 1 corresponded to a time-domain velocity signal of 1 deg/s in amplitude at 1 Hz (scaling included normalizing out the Hann window's effect on spectral magnitude, by using the sum of the taps of the Hann window's impulse response). For each data segment, the phase of the eye movements was computed as the phase of the segment's Fourier transform minus the phase of the Fourier transform of the stimulation in the same data segment.

In order to improve the overall spectral estimate, spectra from the segments were combined using the averaged complex spectrum. The complex spectra from each segment were averaged, and from that Cartesian average, the magnitude was computed. This eliminated the bias of averaging only the spectral magnitudes. Similarly, the phase calculated from the Cartesian average gave a consistent estimate, in contrast to the phase calculated from averaging only the phases of segment spectra.

Results

VOR FREQUENCY RESPONSE TESTS WITH 250 PPS

Time plots in figure 3.2 show eye movements in guinea pig "D", in response to electrical stimulation at 250 pps. The square wave patterns at the bottom of the plots indicate when stimulation was applied. There was little eye movement activity prior to stimulation. Once stimulation commenced, the eye movements were clearly phase-locked to the modulated stimulation. With 1.5 Hz modulation, horizontal eye movements at 1.5 Hz were clearly visible (figure 3.2A). Similarly, for 7 Hz modulation, horizontal eye movements at 7 Hz were clearly visible (figure 3.2C). Horizontal eye movements were much more evident than vertical eye movements (figure 3.2B and 3.2D), as expected since the electrode tip was placed in the lateral canal.

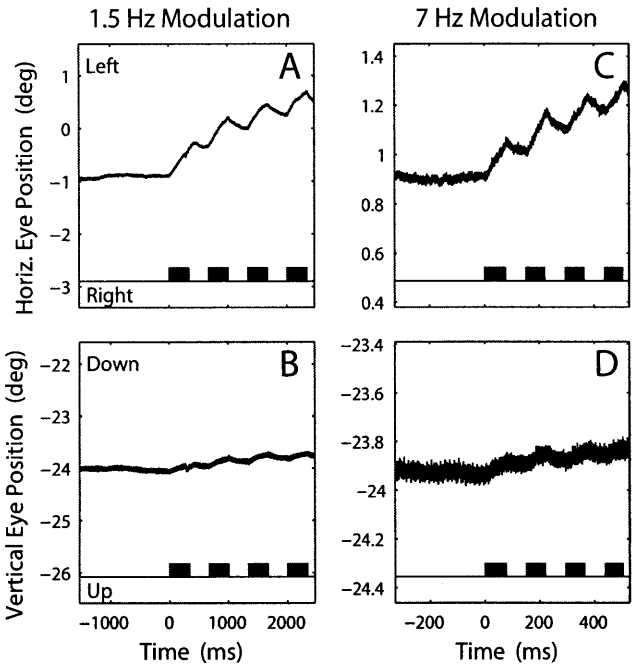

Figure 3.2. Time plots of eye position in response to electrical stimulation for guinea pig "D", using 250 pps stimulation. The square wave patterns near the bottom of the plots indicate the time when stimulation was given. (A) and (B) show an experiment with 1.5 Hz modulation. Stimulation in the right ear caused slow phase eye movements to the left, as expected. The effect was much greater in horizontal eye movements (A) compared to vertical eye movements (B), as expected, because the electrode was inserted in the ampulla of the lateral canal during surgery. (C) and (D) show similar results in an experiment with 7 Hz modulation.

Figure 3.3 shows spectra of stimulation and horizontal eye movements. When the modulation was 7 Hz, figure 3.3A shows that the stimulation had the expected pattern of spectral peaks at odd harmonics of the fundamental frequency, and with amplitude varying inversely with frequency. For a linear system, the output is expected to have components at the same frequencies as the input. Indeed, figure 3.3B shows that the horizontal eye velocity signal had clear spectral peaks at 7, 21, 35, 49, and 63 Hz. At higher frequencies, the peaks do not rise clearly above the noise floor.

When the modulation frequency was 123 Hz, figure 3.3C shows that the stimulation had a spectral peak at 123 Hz and another peak at 127 Hz, at the same amplitude. This is the spectral replication about the 250 pps biphasic pulse rate (127 = 250 - 123). Figure 3.3D shows that the horizontal eye velocity signal had peaks at the same frequencies.

Figure 3.4 compares spectral responses at the fundamental modulation frequency to responses at higher harmonics. Figure 3.4A shows guinea pig "S" eye movement responses at the fundamental modulation frequency, as well as at the 3rd and 5th harmonics of the modulation frequency. The latter responses are scaled up by factors of 3 and 5 respectively, to make them comparable to the response at the fundamental frequency, since the strength of the harmonics in the stimulation varied inversely with frequency. For figure 3.4, components were only included if they had a clear peak above the surrounding noise floor, judged by eye. Responses from all these harmonics were consistent with each other – for all harmonics, the response increased to a peak near 50 Hz, and then decreased.

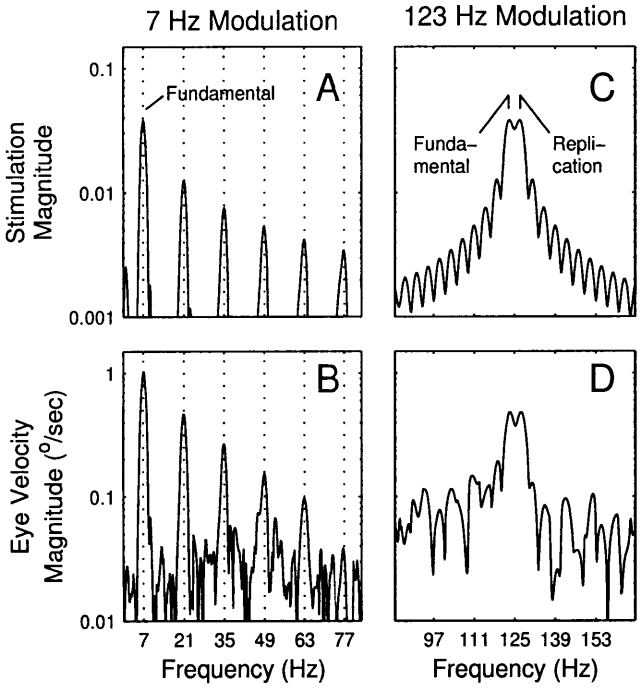

Figure 3.3. Spectra of stimulation and horizontal eye velocity. (A) With 7 Hz modulation, the stimulation has components at odd multiples of 7 Hz, and the amplitude of the components varies inversely with frequency. (B) The spectrum of the horizontal eye velocity signal also has spectral peaks that are clearly above the noise at 7, 21, 35, 49, and 63 Hz. At higher frequencies, spectral peaks are not clearly above the noise floor. (C) For 123 Hz modulation, the stimulation has a component at the fundamental frequency of 123 Hz, and also a component at 127 Hz (250-123). (D) The horizontal eye velocity spectrum also has components at 123 and 127 Hz, as expected for a linear system.

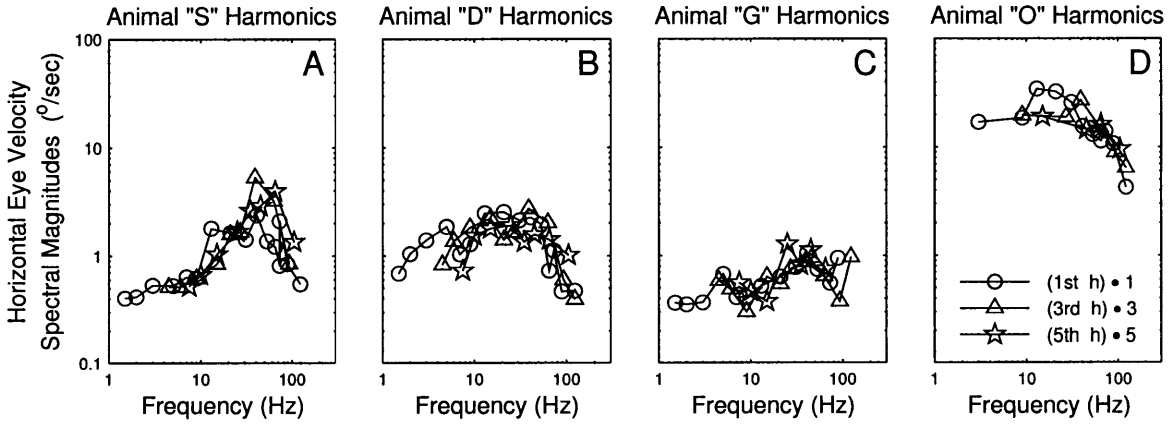

Figure 3.4. Responses at the first (o), third (Δ), and fifth (★) harmonics. Panel (A) shows results for guinea pig "S", panel (B) shows results for animal "D", panel (C) shows results for animal "G", and panel (D) shows results for animal "O". Responses at the fundamental frequency (o) were used to sweep out a frequency response. Square wave modulated stimulation has components at odd harmonics of the fundamental frequency, and the strength of these components varies inversely with frequency. Therefore, responses at the third harmonics were scaled up by a factor of 3. Similarly, responses at the fifth harmonics were scaled up by a factor of 5. For these harmonics, points were plotted only if they had a peak clearly above the noise floor. The frequency magnitude responses of the higher harmonics was similar to the response of the fundamental, consistent with linear system dynamics.

Beyond the 5th harmonic, a similar consistent pattern in all animals was also seen in all higher harmonics that had a clear spectral peak above the surrounding noise floor. Since responses from these harmonics are consistent with each other, this is consistent with linearity and time-invariance in the dynamics of the central VOR as tested here.

Based on the consistency of responses at higher harmonics, frequency response graphs (figure 3.5) were created by combining spectral response data from experiments at different modulation frequencies. Starting with the fundamental, successive odd harmonics of each modulation frequency were included if they had a clear peak above the surrounding noise floor, judged by eye. The additional points from higher harmonics give a much fuller graph and substantially clarify the patterns in the results. Above 151 Hz, the eye movements did not have spectral peaks that were above the noise floor.

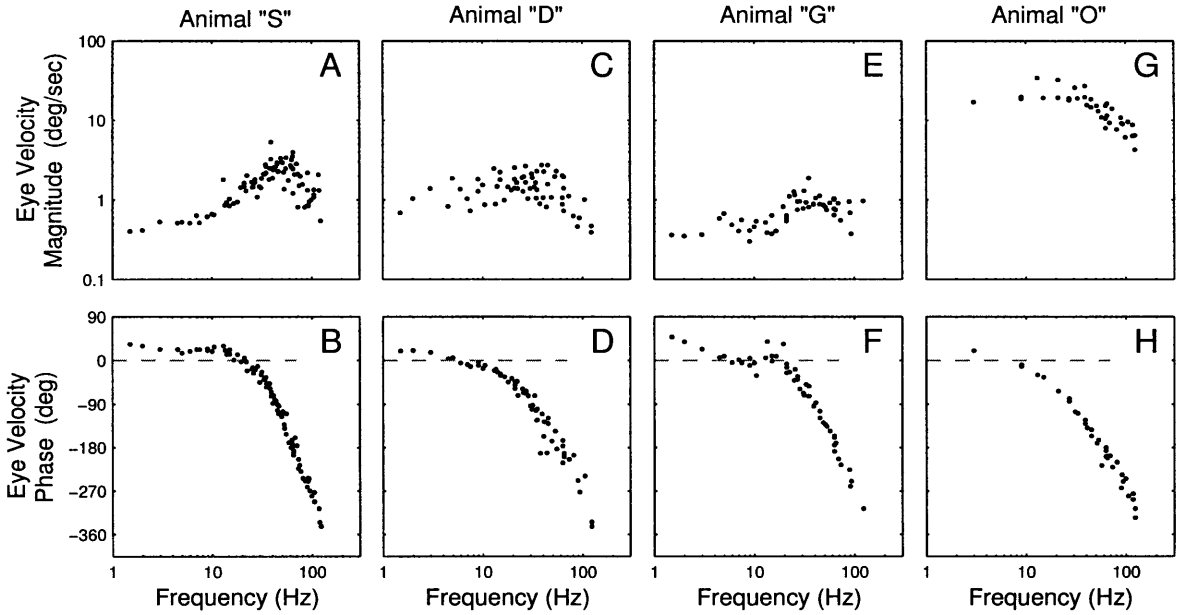

Figure 3.5. Frequency responses using 250 pps. Panels (A), (C), (E), and (G) show magnitude responses for guinea pigs "S", "D", "G", and "O" respectively. These plots show all consecutive harmonics for which there was a peak clearly above the noise floor. As in figure 3.4, these peak magnitudes were multiplied by the harmonic number, to make them comparable to one another. The magnitude responses are fairly flat up to 8 Hz, increase to a peak near 50 Hz, and then fall off at higher frequencies. Panels (B), (D), (F), and (H) show corresponding unwrapped phase responses. In all phase responses, the predominant feature is the increase in phase lag as a function of frequency, consistent with the effect of pure delay in the simple VOR. At low frequencies there is a phase lead (the dashed gray line shows a phase of 0°).

Figure 3.5A shows the magnitude response for guinea pig "S". The magnitude response is fairly flat from 1.5 to 8 Hz, and then increases to a peak near 50 Hz, before falling off at higher frequencies. The magnitude response from 1.5 to 151 Hz is constant within an order of magnitude, compared to a first order filter response which would fall

off by two orders of magnitude over the same frequency range. The unwrapped phase[3] response for animal "S" is shown in figure 3.5B. At low frequencies, there is a small phase lead. At higher frequencies, there is a phase lag, and the lag clearly increases with frequency, consistent with the effect of pure delay[4] in the simple VOR. Similar responses were measured in animal "D" (figures 3.5C and 3.5D), in animal "G" (figures 3.5E and 3.5F), and in animal "O" (figures 3.5G and 3.5H).

VOR Frequency Response Tests with 598 pps

The frequency responses from 598 pps stimulation are shown in figure 3.6. The magnitude and phase responses from guinea pig "S" (figures 3.6A and 3.6B) were very similar to the responses using 250 pps stimulation (figures 3.5A and 3.5B). This was also the case for animal "D" (figures 3.6C and 3.6D) and for animal "G" (figures 3.6E and 3.6F). Responses from guinea pig "O" are not shown in figure 3.6 because when 598 pps stimulation was used, guinea pig "O" had many quick phases, and there were not enough data segments available for averaging.

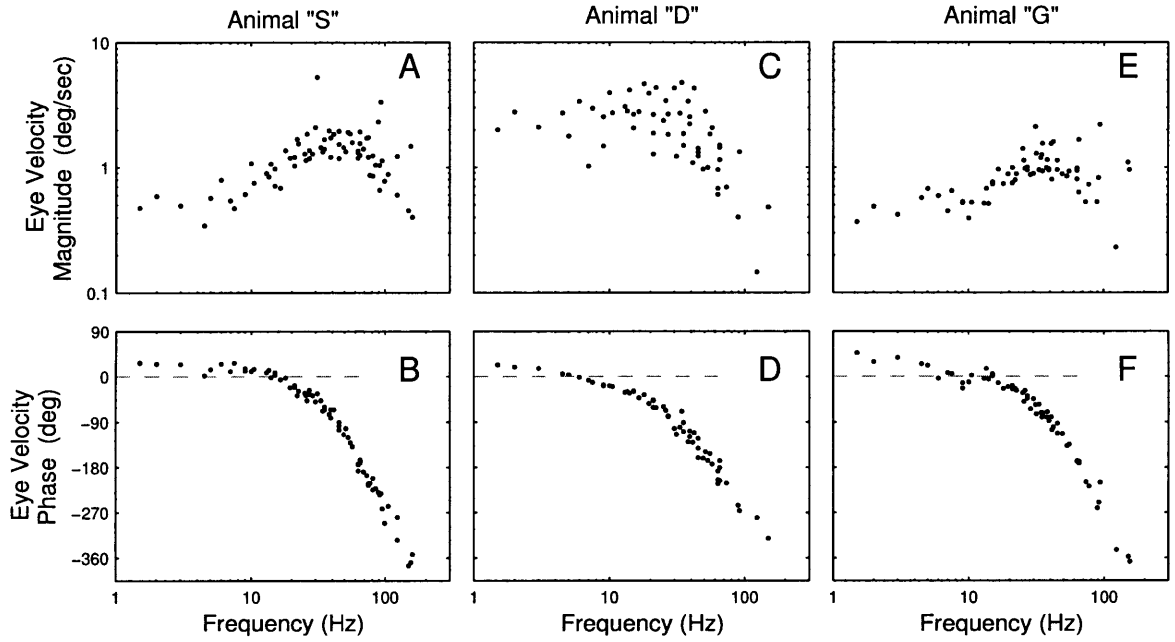

Figure 3.6. Frequency responses using 598 pps. Magnitude plots in panels (A), (C), and (E) are constant within about an order of magnitude, and increase between 8 Hz and 50 Hz. As in figure 3.5, data points consist of all consecutive odd harmonics from each modulation frequency that had a clear peak above the surrounding noise floor. Phase plots in panels (B), (D), and (F) show a clear phase lag that increases with frequency, consistent with the effect of pure delay in the simple VOR. At low frequencies there is a phase lead (the dashed gray line shows a phase of 0°).

[3] The unwrapped phase is the phase, adjusted to eliminate discontinuities of 360 degrees or more

[4] A pure delay is a simple time delay, i.e. a delay of T has Laplace transform of $\exp(-sT)$

MODEL OF FREQUENCY RESPONSE

Guinea pig frequency responses were compared to predictions from modeling the input-output characteristics of the oculomotor plant, VOR central processing, and delay. This was the same model we used for the squirrel monkey (Saginaw et al. 2009).

For the oculomotor plant, we used Robinson's 4th order linear model (Robinson 1964) with the following transfer function:

$$\frac{\theta(s)}{\Delta R(s)} = \frac{sT_z + 1}{(sT_1 + 1)(sT_2 + 1)(sT_3 + 1)(sT_4 + 1)} \quad (1)$$

where s is the Laplace variable, ΔR is the fluctuation of the oculomotor firing rate above or below its baseline rate, and θ is the eye position.

The model for central processing includes a direct path and, in parallel, an integrated path. Thus the transfer function for central processing is $\tau + (1/s)$. If $\tau = T_1$ then the central processing system zero cancels the dominant pole of the plant (the pole with the longest time constant), compensating for the plant's sluggishness. The value of τ used in the central processing network corresponds to a break frequency of 0.57 Hz. Since that is low compared to the frequency range of 1.5 to 293 Hz tested in experiments, the direct path plays the predominant role and the integrated path plays a minor role, because the neural integrator's magnitude response scales inversely with frequency.

The model consists of the central processing network followed by the oculomotor plant. A pure delay term, $\exp(-sT_d)$, is also included to model the delays due to synaptic neurotransmitter release and neural conduction (Robinson 1981, Minor et al. 1999).

Figure 3.7 shows frequency response data along with model response curves. For data sets, the magnitude responses have been scaled to make the mean equal to 1, to facilitate comparison of results from different electrode preparations. The frequency responses obtained using 250 pps were then averaged, using a Cartesian average incorporating magnitude and phase. Responses using 598 pps were similarly scaled and averaged.

In figure 3.7, the dashed blue curves show the responses of the model with parameters from the literature. The plant model is based on Robinson's work with humans, but parameter values have been adjusted for rhesus monkeys (Fuchs et al. 1988) and squirrel monkeys (Minor et al. 1999), which we used, since the squirrel monkey eye is approximately the same size as the guinea pig eye (we use 11 mm eye coils to instrument both species). The following parameter values were used: T_z=0.14, τ=T_1=0.28, T_2=0.037, T_3=0.003, and T_4=0.0004 seconds. We then chose T_d = 0.004 seconds to fit the phase response.

In figure 3.7A, the model magnitude response fits the data within a factor of about 3 at both low and high frequencies. Figure 3.7B shows that the model phase response fits the data well, both in the low frequency phase lead and the high frequency phase lag. However in the magnitude response, the model does not fit the detailed shape of the data in the region near 50 Hz, perhaps because the model parameters were estimated in different species and using data at much lower frequencies than in the present data set.

The data appear to exhibit a resonance near 50 Hz. This is similar to the models of both Robinson (Robinson 1968) and Thomas (Thomas 1967), which used a resonant pair for the upper two poles in their models of the human eye plant, having undamped natural resonant frequencies at 38 Hz and 52 Hz respectively. Therefore, we adjusted

the model by combining the two highest frequency poles into a resonant pair with a peak near 50 Hz. The resonant pole pair had imaginary parts at ±55 Hz and real parts at -20 Hz[5]. The solid red curves in figure 3.7 show the fit with the adjusted parameters. The fit of both the magnitude and phase curves are improved in the region near 50 Hz. For both the literature and adjusted models, the strongly low-pass characteristic of the oculomotor plant cuts off responses above 150 Hz, in agreement with the data.

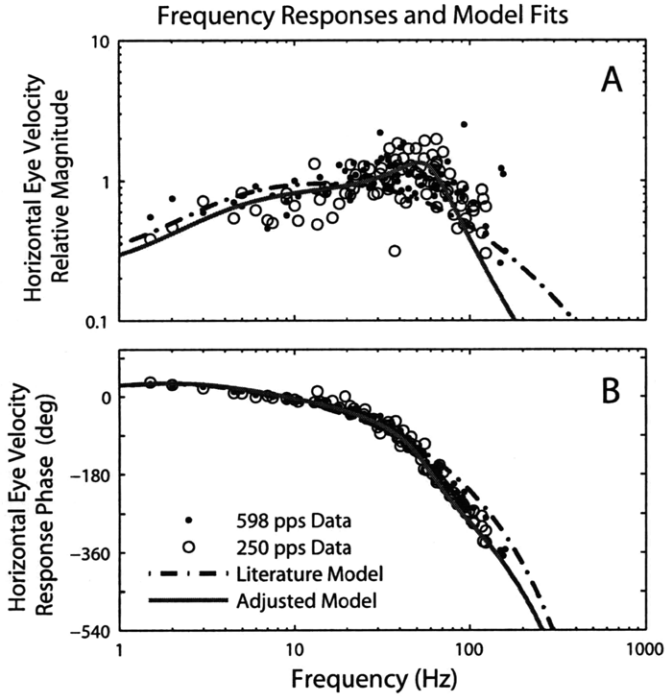

Figure 3.7. Model fits. From experiments using 250 pps, data from guinea pigs "S", "D", "G", and "O" were scaled and averaged (o). From experiments using 598 pps, data from guinea pigs "S", "D", and "G" were scaled and averaged (•). The dashed blue curves show the response of the model using parameter values from the literature, which has all real poles for the guinea pig. For the solid red curves, the two highest frequency poles have been combined into a resonant pair with a maximum magnitude response at 51.2 Hz (see text for all parameter values).

Discussion

Using peripheral electrical stimulation, we have measured the angular VOR in the guinea pig at much higher frequencies than are practical to apply by physically rotating subjects. We have shown that the VOR response is found well above 25 Hz, even though the oculomotor plant is strongly low-pass. The VOR phase response showed a clear lag with frequency, consistent with the effect of pure delay in the simple VOR.

It is important to note that our results are frequency responses from extracellular electrical stimulation with pulses of constant current amplitude. These probably recruit the same afferent population. In contrast, when physical rotation is used, stimulation at different velocities recruits different afferents with different thresholds and dynamics.

One question we sought to address was whether VOR responses could be transmitted above 400 spikes/s, which is the maximum neural firing rate in the

[5] In other words, the peak magnitude response for this pole pair occurred at 51.2 Hz, the damping ratio was ξ=0.342, and the undamped natural frequency was f_n=58.5 Hz

peripheral vestibular nerve (Goldberg and Fernandez 1971, Fuchs et al. 1988). Responses might be transmitted above 400 Hz if parallel pathways were stimulated asynchronously. We used stimulation at 598 pps, well above the maximum peripheral firing rate, and the highest frequency at which we measured responses that were clearly above the spectral noise floor was 151 Hz. Thus our data can't be used to address the question of asynchronous responses in the guinea pig.

Magnitude Response of VOR

The VOR magnitude response was approximately constant from 1.5 to 8 Hz, increased to a peak near 50 Hz, and decreased at higher frequencies. The magnitude response was constant within an order of magnitude from 1.5 to 151 Hz, compared to a first order filter response which would fall off by more than two orders of magnitude over the same frequency range. These results cannot be compared with results from physical rotation of guinea pigs, because there is little overlap in the range of frequencies studied (Escudero et al. 1993; Andrews et al. 1997; Pettorossi et al. 1986).

We attribute the fall-off in the magnitude response above 50 Hz to the strongly low-pass nature of the oculomotor plant, which is modeled by a transfer function with four poles and only a single zero. The response resonance occurred at substantially lower frequency in the guinea pig than in the squirrel monkey (Saginaw et al. 2009). We attribute this to the fact that the squirrel monkey makes quicker body movements, and hence needs to make quicker VOR eye movements.

In guinea pig "O" the shape of the frequency response was similar to the other three guinea pigs, but the eye velocities were an order of magnitude larger than the other animals. Responses for each animal were dependent on electrode placement, and we believe this caused the difference in the magnitude of the eye velocities. We are surprised, however, that the response in guinea pig "O" was so much bigger than in the other animals.

Phase Response of VOR

In the phase response, there was a low frequency phase lead and a pronounced high frequency phase lag. Both of those are matched by predictions of the model. The low frequency phase lead is in agreement with the effect of the system zero in the model of the oculomotor plant. The high frequency phase lag is caused by two factors: (1) primarily by the 4 ms pure delay in the three-neuron arc of the simple VOR, and (2) partially by the 180 degree phase lag coming from the model transfer function, which has four poles and only two system zeros. The same pure delay was also found in the squirrel monkey (Saginaw et al. 2009), and a similar delay for the VOR was also measured in another study (Merfeld et al. 2006).

When physical rotation has been used to study the VOR in rhesus monkeys, a similar phase lag has been found from 25 to 50 Hz (Ramachandran and Lisberger 2005). However, in the range from 10 to 25 Hz, studies using physical rotation have not found significant phase lag (Minor et al. 1999; Huterer and Cullen 2002; Ramachandran and Lisberger 2005). The lag effect of the VOR pure delay may be cancelled by the phase lead of the canal afferents (Fernandez and Goldberg 1971). Those dynamics are included when physical rotation is used, whereas they are intentionally bypassed by our electrical stimulation.

CONTROL TESTS AND ARTIFACTS

In the companion paper (Saginaw et al. 2009), control tests verified that squirrel monkey eye movements up to 267 Hz were predominantly physiological, rather than artifactual. Since the same search coil system was used, the eye coils had the same diameter and number of turns, and the proximity of the electrode to the eye coil was similar, we attribute our guinea pig results from 1.5 to 151 Hz to physiological results, rather than artifacts.

CONCLUSIONS

The central angular VOR in the guinea pig has a frequency response that extends well above 2 Hz explored in previous studies, and is found up to 151 Hz. We do not believe the response has an ecologic function at such high frequencies. Nevertheless, this work shows that the nervous system is capable of transmitting modulated signals up to at least 151 Hz, supporting the viability of vestibular prostheses that use stimulation modulated around a baseline rate that is substantially higher than the guinea pig spontaneous rate of 30-60 spikes/s. This work also demonstrates that eye movements can be measured up to 151 Hz, even though the oculomotor plant has strongly low-pass characteristics.

In the magnitude response, the roll-off above 50 Hz is consistent with the low-pass nature of the oculomotor plant, which is modeled by a transfer function with four poles and only a single zero. The resonance in the guinea pig response is at a lower frequency than in the squirrel monkey, because the squirrel monkey makes quicker body movements and hence needs to make quicker eye movements.

In the phase response, the phase lag is consistent with the effect of pure delay in the three-neuron arc of the simple VOR. In fact, the pure delay in the guinea pig is the same as in the squirrel monkey, since the mechanisms of neurotransmitter latency and signal conduction along the three-neuron arc are very similar in both species.

Acknowledgements

We thank Richard Lewis for eye coil surgeries, Jennifer Morrissey for assistance with the animals, and Margaret Lankow for administrative support. We appreciate the helpful comments from M. Saginaw's thesis committee: Charles Oman, Louis Braida, Richard Lewis, and Steve Massaquoi. The material in this paper is a portion of a doctoral thesis (Saginaw 2010) submitted to the Department of Electrical Engineering and Computer Science, Massachusetts Institute of Technology, Cambridge MA, in partial fulfillment of requirements for the degree of Doctor of Philosophy.

Grants

Support from NIH F31 DC006202, R01 DC03066, and R01 DC008167, and European Commission 225929 gratefully acknowledged.

References

Andrews JC, Koyama S, Li J, Hoffman LF. Vestibular and optokinetic function in the normal guinea pig. *Ann Otol Rhinol Laryngol* 106: 838-847, 1997.

Della Santina CC, Migliaccio AA, Patel AH. A multichannel semicircular canal neural prosthesis using electrical stimulation to restore 3-D vestibular sensation. *IEEE Trans Biomed Eng* 54, 1016-1030, 2007.

Escudero M, de Waele C, Vibert N, Berthoz A, Vidal PP. Saccadic eye movements and the horizontal vestibulo-ocular and vestibulo-collic reflexes in the intact guinea-pig. *Exp Brain Res* 97: 254-262, 1993.

Fernandez C., Goldberg JM. Physiology of peripheral neurons innervating semicircular canals of the squirrel monkey. II. Response to sinusoidal stimulation and dynamics of peripheral vestibular stimulation. J Neurophysiol 34: 661-675, 1971.

Fuchs AF, Scudder CA, Kaneko CRS. Discharge patterns and recruitment order of identified motoneurons and internuclear neurons in the monkey abducens nucleus. *J Neurophysiol* 60: 1874-1895, 1988.

Goldberg JM, Fernandez C. Physiology of peripheral neurons innervating semicircular canals of the squirrel monkey. I. Resting discharge and response to constant angular accelerations. J Neurophysiol 34: 635-660, 1971.

Gong W, Merfeld DM. Prototype neural semicircular canal prosthesis using patterned electrical stimulation. *Ann Biomed Eng* 28: 572-581, 2000.

Gong W, Merfeld DM. System design and performance of a unilateral horizontal semicircular canal prosthesis. *IEEE Trans Biomed Eng* 49, 175-181, 2002.

Huterer M, Cullen KE. Vestibuloocular reflex dynamics during high-frequency and high-acceleration rotations of the head on body in rhesus monkey. *J Neurophysiol* 88: 13-28, 2002.

Merfeld DM, Gong W, Morrissey J, Saginaw M, Haburcakova C, Lewis RF. Acclimation to chronic constant-rate peripheral stimulation provided by a vestibular prosthesis. *IEEE Trans Biomed Eng* 53: 2362-2372, 2006.

Minor LB, Lasker DM, Backous DD, Hullar TH. Horizontal vestibuloocular reflex evoked by high-acceleration rotations in the squirrel monkey. I. Normal responses. *J Neurophysiol* 82: 1254-1270, 1999.

Paige G. Vestibuloocular reflex and its interactions with visual following mechanisms in the squirrel monkey. I. Response characteristics in normal animals. *J Neurophysiol* 49: 134-151, 1983.

Pettorossi VE, Bamonte F, Errico P, Ongini E, Draicchio F, Sabetta F. Vestibulo-ocular reflex (VOR) in guinea pigs. *Acta Otolaryngol* 101: 378-388, 1986.

Ramachandran R, Lisberger SG. Normal performance and expression of learning in the vestibulo-ocular reflex (VOR) at high frequencies. *J Neurophysiol* 93: 2028-2038, 2005.

Robinson DA. A method of measuring eye movement using a scleral search coil in a magnetic field. *IEEE Trans Biomed Eng* 10: 137-145, 1963.

Robinson DA. The mechanics of human saccadic eye movement. *J Physiol* 174: 245-264, 1964.

Robinson DA. The oculomotor control system: A review. *Proc IEEE* 56: 1032-1049, 1968.

Robinson DA. The use of control systems analysis in the neurophysiology of eye movements. *Ann Rev Neurosci* 4: 463-503, 1981.

Saginaw MA. *Eye Movement Studies with a Vestibular Prosthesis* (Ph.D. Thesis). Cambridge MA: Massachusetts Institute of Technology, 2009.

Saginaw MA, Gong W, Haburcakova C, Merfeld DM. Angular vestibulo-ocular reflex above 100 Hz elicited by electrical stimulation of the vestibular peripheral nerve. I. responses in the squirrel monkey. *J Neurophysiol to be submitted 2009*.

Thomas JG. The torque-angle transfer function of the human eye. *Kybernetik* 3: 254-263, 1967.

Chapter 4

Attenuation of Eye Movements Evoked by a Vestibular Implant at the Frequency of the Baseline Pulse Rate

Michael A. Saginaw, *Student Member, IEEE*, Wangsong Gong, Csilla Haburcakova, and Daniel M. Merfeld, *Member, IEEE*

***Abstract*—We are developing a vestibular implant to electrically stimulate vestibular neurons in the semicircular canals in order to alleviate vertigo, which is a commonly occurring problem. However, since electrical stimulation causes synchronous (phase-locked) neural responses, such electrical stimulation might also cause inappropriate vestibulo-ocular eye movements and visual blurring. We investigated this in the guinea pig using electric stimulation with a constant rate of 250 pulses per second, and measured eye movements at 250 Hz with a velocity of 8.1 deg/sec, which might cause visual blurring. However, after half an hour of stimulation, that component reduced to 1.6 deg/sec. The average time constant for this reduction was 5.0 minutes. After one week of constant stimulation, the 250 Hz response component was only slightly smaller, at 1.2 deg/sec. We conclude that although an electrical prosthesis with a resting rate of 250 pulses per second may cause some visual blurring when first turned on in a human patient, such blurring is very likely to attenuate and be imperceptible within several minutes, and therefore does not appear to pose a serious long-term problem.**

***Index Terms*—Biomedical engineering, Prosthetics, Translational medicine, Vestibulo-ocular reflex**

I. Introduction

DIZZINESS and imbalance are commonly occurring problems that are often caused by disorders of the vestibular system. Vestibular dysfunction can make people much more likely to suffer falls, which can have severe detrimental consequences for an individual's life [1]. Vertigo is also a debilitating effect of Meniere's syndrome.

Inner ear problems may be the result of malfunction of vestibular hair cells, which can be caused by certain antibiotics, or by ion imbalances in inner ear endolymph and perilymph fluids. All of these peripheral problems

Manuscript to be submitted 2009. This work was supported in part by the U.S. Department of Department of Health and Human Services under NIH Fellowship F31 DC006202, NIH Grants R01 DC03066, and R01 DC008167, and European Commission 225929.

M. A. Saginaw is with the.Jenks Vestibular Physiology Laboratory, Massachusetts Eye and Ear Infirmary, Room 421, 243 Charles St, Boston MA 02114 USA (phone: 617-573-6494, fax: 617-573-5502, email: MSaginaw@alum.mit.edu). He is also with the Department of Electrical Engineering and Computer Science, Massachusetts Institute of Technology, Cambridge MA

W. Gong is with the.Jenks Vestibular Physiology Laboratory, Massachusetts Eye and Ear Infirmary, Boston MA 02114 USA. He is also with the Department of Otology and Laryngology, Harvard Medical School, Boston MA 02114 USA (email: Wangsong_Gong@meei.harvard.edu)

C. Haburcakova is with the.Jenks Vestibular Physiology Laboratory, Massachusetts Eye and Ear Infirmary, Boston MA 02114 USA. She is also with the Department of Otology and Laryngology, Harvard Medical School, Boston MA 02114 USA (email: Csilla_Haburcakova@meei.harvard.edu)

D. M. Merfeld is with the.Jenks Vestibular Physiology Laboratory, Massachusetts Eye and Ear Infirmary, Boston MA 02114 USA. He is also with the Department of Otology and Laryngology, Harvard Medical School, Boston MA 02114 USA (email: Dan_Merfeld@meei.harvard.edu)

interfere with the vestibular system's ability to transduce head motion into a neural afferent signal.

Since the vestibular periphery can become faulty, we are developing an electrical prosthesis that bypasses the usual transduction processes and provides information about head motion and orientation to the vestibular nerve. The device is analogous to a cochlear implant, which provides auditory information to the cochlear nerve.

We have been testing the vestibular prosthesis in laboratory animals. Thus far the prosthesis effectiveness has been assessed primarily by measuring eye movements. The vestibulo-ocular reflex (VOR) functions in healthy individuals to maintain steady gaze when the head moves. Similarly, prosthetic stimulation should evoke eye movements appropriate for motion indicated by the stimulation. Results are promising, and the prosthesis can restore a significant amount of VOR function [2-8]. However, electrical stimulation is known to elicit synchronous neural responses that are phase-locked to the stimulation [9]. Normally the parallel paths in the VOR neural networks are believed to operate asynchronously, so that instantaneous effects of any one path are averaged and smoothed in the ensemble. However if the paths are phase locked, this may cause synchronized jerks or twitches in the eye movements, which in turn may cause visual blurring. Here, we investigate this potential side-effect using the guinea pig as our animal model.

II. Methods

A. Animal Preparations

Three mature (> 700 g), male, pigmented guinea pigs (*Cavia porcellus*), referred to as animals "S", "D", and "O", were used as subjects. All work with animals adhered to a protocol approved by the Institutional Animal Care and Use Committee of the Massachusetts Eye and Ear Infirmary. During all surgeries, guinea pigs were under Isoflurane general anesthesia, and sterile biocompatible materials and aseptic techniques were used. The surgeries have been described elsewhere [2-3, 10], so here only a brief description is given. The three procedures done during surgeries were (1) attaching a head bolt and head cap to house electronics, (2) attaching an eye coil to measure eye movements, and (3) implanting an ear electrode to provide stimulation.

To attach a head bolt, skin was resected on top of the head to expose the skull. The skull was drilled, and inverted titanium screws were placed under the skull just above the dura, and rotated 90 degrees to secure them in place. A head bolt made of composite ("G10") was placed between the screws and held very securely in place by the combination of the screws and dental acrylic. The head bolt was used to secure the head cap, an enclosure measuring approximately 44x34x33 mm and also made of G10. The head cap housed the stimulator electronics.

To attach an eye coil, the conjunctiva was resected and an 11 mm diameter 3-turn coil was placed on the sclera. Coils were made of stainless steel Cooner Wire AS632 (Cooner Wire, Inc., Chatsworth, CA). Standard methodology was used [11]. Eye coil leads were brought subcutaneously to the head cap, making them inaccessible to the animal.

An electrode was implanted in the ear, to stimulate neurons innervating the lateral semicircular canal. An incision was made behind the ear to expose the canals. A hole was drilled in the bony wall, and an electrode was inserted so that the tip was in the vicinity of the ampulla of the lateral canal. Electrodes were made of 150 μm diameter Teflon coated platinum Cooner Wire AS770-40, with approximately 100-200 μm of insulation stripped at the tip. Additional details on the electrode are described elsewhere [2]. The fine positioning of the electrode was adjusted using a micromanipulator until electric stimulation elicited primarily horizontal eye movements. At that point, the stimulating electrode was secured in place using a stainless steel screw and dental acrylic, and the hole in the canal was sealed with bone wax.

The return electrode was made of the same type of wire as the stimulating electrode, but with about 2 mm of insulation stripped at the end. The return electrode was placed securely in superficial neck musculature near the stimulated ear. Electrode leads were brought subcutaneously to the head cap and were inaccessible to the animal.

In guinea pigs "D" and "O", the lateral semicircular canal was also plugged. Plugging was done since some animals were also used in motion testing unrelated to the studies reported here. Canal plugging should not

affect the experiments reported here, because this study does not involve motion of the animals, and canal plugging has little to no effect on the spontaneous firing rate of the vestibular afferents [12-13]. This was confirmed by our data, which showed similar responses with and without canal plugging. In addition, electrode insertion causes deposit development around the electrode tip [14], causing some blockage of the fluid flow in the canal, and plugging the canal makes certain that the canal is blocked. Canal plugging was done using standard methods [13].

B. Experiments

During tests, animals were stationary. The head was pitched forward at approximately 45° to align the lateral canals with earth-horizontal, and held motionless via the head cap. All data were acquired in the dark (except where noted otherwise), in order to focus on vestibularly driven eye movements.

Stimulation consisted of biphasic pulses with a 200 μs stimulatory (cathodic) phase, followed by a 200 μs rest phase, followed by a 200 μs inhibitory (anodic) phase. A current source was used in order to control charge delivery. A voltage source would not control charge delivery accurately, due to time-varying impedances in animal tissue [15-16]. Thus charge delivery was balanced, in order to reduce dissolution of the electrode and damage to tissue [17].

Stimulation current amplitude was adjusted for each animal, because exact electrode placement in surgery was different for each animal. Stimulation amplitude was adjusted to be large enough to elicit substantial eye movements, but kept low enough to avoid causing facial nerve stimulation and facial twitching. Amplitudes ranged from 60 to 125 μA. The stimulation rate was 250 pulses per second (pps).

Eye movements were measured by the eye coil, in conjunction with a search coil system. During all tests the animal was positioned with its eyes at the center of a Robinson-style [18] search coil system (CNC-Engineering, Seattle WA), which generated magnetic fields at 108 kHz and 72 kHz. Horizontal and vertical eye positions were determined from the eye coil voltage, using envelope detection. The horizontal and vertical eye position signals were then filtered by a 5^{th} order Bessel lowpass filter with a -3 dB frequency of 3000 Hz, and sampled at 9000 Hz using a 16 bit analog to digital converter card by National Instruments, and transferred to a computer using LabView (both by National Instruments, Austin TX). The data were stored on hard disk for offline processing.

Stimulation was alternately on for one week and off for one week, for a total of eight weeks. Each time a transition was made, stimulation was left in that state for one week, and then switched again. Thus, stimulation was on for weeks 1, 3, 5, and 7.

Eye movements were measured at four times each week: (1) for five minutes prior to the stimulation transition, (2) for 30 minutes, with the transition occurring about 10 seconds after the start of acquisition, (3) for 10 minutes in the light, and (4) for five more minutes. All data were acquired in the dark except as noted. Thus at the end of each week with stimulation, acquisition (1) served to show the effect after a full week of stimulation.

C. Data Analysis

Data were analyzed using MATLAB (The MathWorks, Natick MA). Spectral analysis was carried out using the fast Fourier transform on 2-second non-overlapping data segments. Nystagmic quick phases were not removed from the data because we are interested in the eye response at 250 Hz, and we have shown that quick phases do not affect the spectrum magnitude above 80 Hz for guinea pigs [19]. To reduce bias due to spectral leakage, the data segments were tapered using Hann windows. Eye position data spectra were converted to velocity in the frequency domain via multiplication by a frequency ramp. Amplitudes were scaled such that a spectral magnitude of 1 at 1 Hz corresponded to a time-domain signal of 1 deg/sec in amplitude.

The exponential curve, $A \cdot \exp(-t/\tau) + B$, was fit to the data from the first half hour after stimulation was turned on. The parameters A, B, and τ were optimized to minimize the absolute value of the difference between the curve and the data, using a nonlinear minimization function in MATLAB.

III. RESULTS

When electrical stimulation at 250 pps was first delivered to the vestibular nerve in the lateral canal, there was a sizable 250 Hz component in the horizontal eye movements. Fig. 4.1 shows horizontal eye movement spectra for guinea pig "O". Panel (A) shows that when stimulation was first turned on, there was a clear 250 Hz component, with a magnitude of 10.3 deg/sec. Also when stimulation was first turned on, there was very substantial saccadic activity, with approximately 8 nystagmic beats per second, as reflected in the spectrum in the vicinity of 8 Hz. In contrast, panel (B) shows that in the absence of stimulation, there was no 250 Hz component, and no spectral activity near 8 Hz.

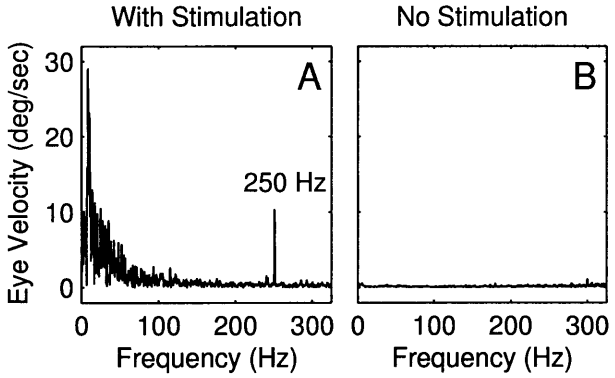

Fig. 4.1. Spectra with and without stimulation. When stimulation with a constant rate of 250 pps was first turned on (A), the horizontal eye velocity spectrum magnitude had a clear component at 250 Hz, with a magnitude of 10.3 deg/sec. There was also spectral energy focused near 8 Hz, which was the rate of nystagmic quick phases when stimulation was first turned on. In contrast, there was no 250 Hz component without stimulation (B).

Fig. 4.2 tracks the time-evolution of the 250 Hz component in all three guinea pigs. Results were similar in each animal and each time the stimulation was turned on (weeks 1, 3, 5, and 7). In all cases, just before stimulation was turned on, there was no 250 Hz component above the noise floor. Right after stimulation was turned on, the 250 Hz component was near 8 to 10 deg/sec. However, during the first half hour of stimulation, the 250 Hz component dropped to about 1 to 2 deg/sec. The animals were in the dark during this time. The fact that the 250 Hz component changed over several minutes shows that the component is not an electromagnetic artifact, since artifacts due to electromagnetic phenomena would exhibit time constants of the order of nanoseconds, rather than minutes.

The 250 Hz component did not change much after the first 30 minutes in the dark. When the animals were in the light for 10 minutes, the 250 Hz component stayed at a similar value slightly below 2 deg/sec. The value was also similar at the end of the week when the animals were retested, just before turning off the stimulation. In other words, very little additional reduction occurred in the 250 Hz component. It should be emphasized that for almost the entire week, the animals were in normal lighting conditions. They were free to move in their cages, and had a full week for visual retinal slip signals to help them reduce inappropriate eye movements, if sensed. Yet even at the end of each week of stimulation, the 250 Hz component, though small, remained above the noise floor.

When stimulation was turned off at the end of weeks 1, 3, 5, and 7, there was no after-effect. An oppositely directed after-effect would have manifested as a positive magnitude on the magnitude plot, but no such response is visible, and this was the case for all animals and for all weeks when stimulation was transitioned to off.

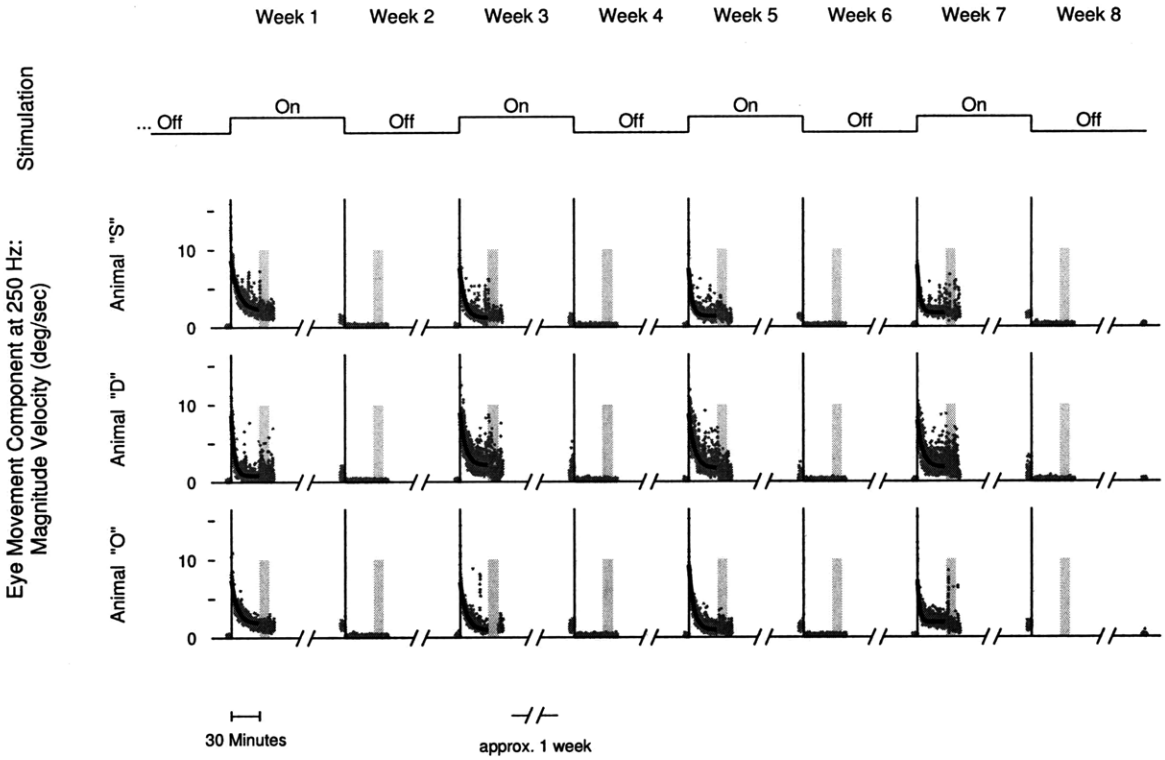

Fig. 4.2. Time evolution of 250 Hz component. Eye movements were measured before, during, and after stimulation transitions. Yellow patches indicate when the animals were in the light. When the stimulation was off, there was no significant component at 250 Hz. When the stimulation was turned on, the 250 Hz component spiked to about 8 to 10 deg/sec, which might yield perceptible blurring for a patient with the prosthesis. However, this component then diminished to about 1.6 deg/sec during the next half hour. There was not substantial reduction during the 10 minutes in the light, during 5 subsequent minutes in the dark, or after the animal spent a week in normal lighting conditions and was then retested for 5 minutes in the dark, right before the next stimulation transition. For the first half hour after stimulation was turned on, an exponential curve, $A \cdot \exp(-t/\tau) + B$, was fit to the data. Fit curves are shown in black. For guinea pig "O", some data were acquired at 200 Hz, and the 250 Hz component could not be analyzed.

The exponential curve, $A \cdot \exp(-t/\tau) + B$, was fit to the data from the first half hour after stimulation was turned on. The exponential curves are shown in black in fig. 4.2.

Fig. 4.3 shows parameter values from the exponential fits. Parameter values were similar in all animals, and for all weeks. Panel (A) shows the curve fit peak velocity, i.e. the value of $A+B$ from the curve fits. These peak values averaged 8.1 deg/sec and were similar for all animals and all weeks. Panel (B) shows the asymptotic final velocity, i.e. the parameter B. These values averaged 1.6 deg/sec and were also consistent for all animals and weeks. Finally, panel (C) shows that the time constants averaged 5.0 minutes and were typically between 3 and 6.5 minutes, so that within half an hour several time constants had passed, and the high peak velocity had decreased to near its final value.

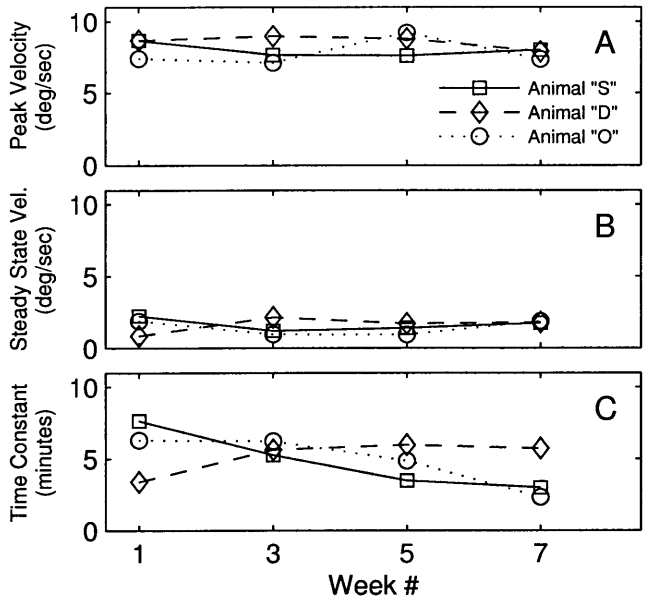

Fig. 4.3. Parameters from curve fitting. The time evolution of the 250 Hz component was fit by an exponential curve, $A \cdot \exp(-t/\tau) + B$, when the stimulation was turned on in weeks 1, 3, 5, and 7. Panel (A) shows the peak fit velocity, i.e. $A+B$. These values averaged 8.1 deg/sec and were similar for all animals and for all weeks when the stimulation was turned on. Panel (B) shows the asymptotic final value of the curve fits, i.e. the parameter B. These values averaged 1.6 deg/sec, and were also consistent for all animals and for all weeks. Panel (C) shows the time constant τ, which averaged 5.0 minutes and was typically between 3 and 6.5 minutes. With this range of time constants, the size of the 250 Hz component dropped to near its small final value within a half hour of turning on the stimulation. None of these parameters shows a clear trend over time as stimulation was turned on successively.

Fig. 4.4 shows that the 250 Hz component was large at the start of stimulation, but under all other conditions it was consistently small. At the start of stimulation, the component averaged 8.1 deg/sec. After a half hour in the dark, the component dropped to an average of 1.6 deg/sec. It remained at a similar level, at an average of 1.7 deg/sec, when tested in the light. For the next week the animals were in the animal care facility in normal lighting conditions. This might be expected to drive adaptation if the retinal slip signal was substantial. However at the end of the week, the 250 Hz component was not greatly altered, and averaged 1.2 deg/sec. In a paired t-test comparing the value at the end of the first half hour to the value during the test in the light, there was no significant difference ($p=0.468$). In a paired t-test comparing the value at the end of the first half hour to the value at the end of the week, the difference was significant at the 95% level ($p=0.031$), but it was a small difference of only 0.38 deg/sec.

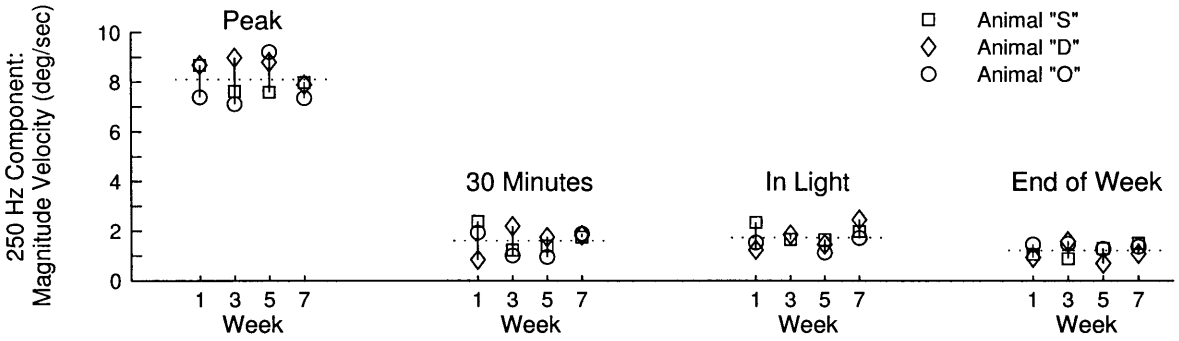

Fig. 4.4. 250 Hz component under different conditions. When stimulation was first turned on ("Peak"), the 250 Hz component averaged 8.1 deg/sec (shown by dotted line). After stimulation was on for 30 minutes, the 250 Hz component dropped to about 1.6 deg/sec. It was at a similar level, 1.7 deg/sec, when the animal was in the light for 10 minutes, and also at a similar level, 1.2 deg/sec, after the stimulation was on for a week. When values at 30 minutes were paired with values in the light for the same animal and week, the differences were not significant (p=0.468). When values at 30 minutes were paired with values at the end of the week, the differences were significant (p=0.031), however the average difference was only 0.38 deg/sec. The magnitude of the 250 Hz component is below the putative visual threshold for all conditions except when the stimulation is first turned on.

IV. Discussion

We have shown that electrical stimulation of the vestibular nerve at a constant rate of 250 pps causes a high frequency eye movement at 250 Hz. Although this component is 8.1 deg/sec when stimulation is first turned on, it drops to 1.6 deg/sec within half an hour while the animal is in the dark, and stays at that low level under a variety of conditions, when the animal is tested in the light, and when it is tested in the dark after a week in normal lighting conditions. When stimulation is turned off, there is no after-effect of a 250 Hz component in the opposite direction of what occurred when stimulation was applied.

In an earlier study, we reported that nystagmus evoked by on/off stimulation transitions showed clear and convincing evidence of dual-state adaptation – with the strength of the nystagmus reduced with each on/off transition [5]. We did not see evidence of such dual-state adaptation in the 250 Hz component. Even when stimulation was turned on for the third or fourth time, the 250 Hz component was as large as the first time stimulation was turned on; none of the animals shifted to a different state. Therefore we project that human patients with the prosthesis will have a similar component at the prosthesis baseline frequency, and this will occur every time the prosthesis is switched on. Since oscillations above 60 Hz exceed the visual fusion frequency [20], if these oscillations are large enough to be perceptible, they would cause visual blurring.

Important issues are whether the component would be perceptible and cause blurring for a human patient, and what mechanism causes the reduction in the component magnitude. These will be discussed in turn.

A. Size of 250 Hz Component and Perception Thresholds

An 8.1 deg/sec amplitude velocity signal at 250 Hz corresponds to a peak-to-peak eye position deviation of 37 arcsec. The 1.6 deg/sec velocity amplitude after 30 minutes of stimulation in the dark corresponds to a peak-to-peak eye position deviation of 7.3 arcsec.

Tremor amplitude in the normal human eye is about the diameter of a cone in the fovea [20]. This

corresponds to approximately 18 arcsec (using 1.5 μm for the diameter of the cone and 17 mm for the focal length [22]). Thus the initial 37 arcsec from the 250 Hz component is larger than the natural tremor, whereas the 7.3 arcsec is smaller. It is not clear if tremor-sized eye movements are important for vision [20].
On the other hand, microsaccades are thought to play a role in vision, and people suppress them when threading a needle or sighting a gun [24]. A typical microsaccade is 300 arcsec.

Another way to assess the size of the 250 Hz component is to compare it to known perceptual thresholds. The center-to-center separation of foveal cones is approximately 2 μm [22], corresponding to 24 arcsec, using the same focal length as above. Human visual acuity is not that precise, due to factors such as diffraction; a person with 20/20 vision can resolve features with a 60 arcsec separation on a Snellen chart [21-22]. However, human visual acuity is better than that for certain perceptual tasks involving straight lines – vernier acuity is approximately 20 arcsec [23]. Thus if humans had initial eye movements of 37 arcsec, they might interfere with the finest human visual tasks, but 7.3 arcsec movements would probably not.

Another indicator of perceptibility is that the size of the 250 Hz component did not decline further while the animal was in the light. It declined to 1.6 deg/sec during the first half hour in the dark. For the next week the animals were in the animal care facility in normal lighting conditions. This might be expected to drive adaptation if the retinal slip signal was substantial. However at the end of the week, the 250 Hz component was not greatly altered, and averaged 1.2 deg/sec. This suggests that the level at the end of the half hour was not interfering with the animal's vision.

B. Component at Stimulation Baseline Rate and Uses of Prosthesis

One possible application of the prosthesis is for Meniere's syndrome. A patient might leave the stimulator off most of the time, and turn it on at the onset of a Meniere's attack, to override the unstable signals generated by their inner ear and stabilize their orientation sensation. In this case the prosthesis would use constant rate stimulation, as was used here. It is likely that the prosthesis would initially elicit eye move movements at the stimulator baseline rate, since that happened every time the prosthesis was turned on in this study. However it is also likely that these eye movements would diminish very quickly compared to a two-day Meniere's attack.

Most prostheses tested so far have been unilateral [2-3, 8], and these especially tend to use a firing rate well above the animal's spontaneous rate, in order to enable the capability of bilateral direction cues. However future work with bilateral or even unilateral prostheses may use lower baseline pulse rates. These would be likely to cause even larger initial eye movement components at the baseline frequency, because the VOR response is larger at those frequencies [10, 19].

C. Mechanism of Reduction of 250 Hz Component

We believe the mechanism of reduction was habituation, rather than central adaptation. We use the definition that habituation is a reduction in response after repeated application of stimulation, whereas adaptation in response to a stimulus is an active change to produce an ecological benefit for the organism [25-26]. We believe the evidence indicates habituation for several reasons.

First, nearly the entire five-fold reduction in the magnitude of the 250 Hz component occurred while the animals were in the dark, with no retinal slip signal to provide a feedback error signal.

Second, a characteristic of adaptation is an oppositely directed after-effect when stimulation stops. We measured no such effect in the 250 Hz component. An oppositely directed after-effect would have appeared as a positive magnitude in fig. 4.2, but no such response was visible, and this was the case for all animals and all weeks when stimulation was turned from on to off. In contrast, an oppositely directed after-effect was measured in guinea pig nystagmus during each on/off transition [5].

Indeed, there were clearly different mechanisms at work in the reduction of the 250 Hz component, and the reduction in nystagmus when stimulation was switched on in [5], because the phenomena happened over very different time scales. The reduction in the 250 Hz component was characterized by a time constant of 5.0 minutes. In contrast, in [5], nystagmic quick phases were prominent when stimulation was first turned on, but they reduced to near the prestimulation baseline over the course of about 1 day.

We speculate that a likely site of habituation is the central processing circuitry of the VOR, based on [27]. They used repeated galvanic stimulation in the region outside the canals, and found no response reduction in the vestibular nerve, very little reduction in the vestibular nuclei (substantial in only 10 of 88 units), and substantial reduction in most eye movement amplitudes. They concluded that the likely site of most habituation was the central processing circuitry of the VOR.

In addition, we did not measure dual state adaptation in the 250 Hz component. Even when stimulation was turned on for the third or fourth time, the 250 Hz component was as large as the first time stimulation was turned on; none of the animals shifted to a different state. In contrast, we did measure dual state adaptation in the nystagmic response; nystagmus diminished markedly by the third time the prosthesis was turned on [5].

D. Conclusions

The main conclusions are that (1) pulsatile electrical stimulation can evoke an eye response at the frequency of stimulation, which may initially cause visual blurring, but that (2) the magnitude of this component will diminish quickly and substantially.

We did not see evidence of dual-state adaptation. Even when stimulation was turned on for the third or fourth time, the 250 Hz component was as large as the first time stimulation was turned on, rather than the animals shifting to a different state. Therefore we project that human patients with the prosthesis might have a similar component at the prosthesis baseline frequency, every time the prosthesis is switched on.

Although an electrical prosthesis may cause some visual blurring when first turned on in a human patient, such a blurring component is very likely to reduce below a perceptible threshold within several minutes, and therefore it does not present a serious problem.

ACKNOWLEDGMENT

We thank Richard Lewis for eye coil surgeries, Jennifer Morrissey for assistance with the animals, and Margaret Lankow for administrative support. We appreciate the helpful comments from M. Saginaw's thesis committee: Charles Oman, Louis Braida, Richard Lewis, and Steve Massaquoi. This paper is a portion of a doctoral thesis (Saginaw 2010) submitted to the Department of Electrical Engineering and Computer Science, Massachusetts Institute of Technology, Cambridge MA, in partial fulfillment of requirements for the degree of Doctor of Philosophy.

REFERENCES

[1] Y. Agrawal, J. P. Carey, C. C. Della Santina, M. C. Schubert, and L. B. Minor, "Disorders of balance and vestibular function in U.S. adults: data from the national health and nutrition examination survey, 2001-2004," *Arch. Intern. Med.*, vol. 169, no. 10, pp. 938-944, May 2009.

[2] W. Gong and D. M. Merfeld, "Prototype neural semicircular canal prosthesis using patterned electrical stimulation," *Ann. Biomed. Eng.*, vol. 28, no. 5, pp. 572-581, May 2000.

[3] W. Gong and D. M. Merfeld, "System design and performance of a unilateral horizontal semicircular canal prosthesis," *IEEE Trans. Biomed. Eng.*, vol. 49, no. 2, Feb. 2002.

[4] R. F. Lewis, W. Gong, M. Ramsey, L. Minor, R. Boyle, and D. M. Merfeld, "Vestibular adaptation studied with a prosthetic semicircular canal," *J. Vestib. Res.*, vol. 12, no. 2-3, pp. 87-94, 2002/2003.

[5] D. M. Merfeld, W. Gong, J. Morrissey, M. A. Saginaw, C. Haburcakova, and R. F. Lewis, "Acclimation to chronic constant-rate peripheral stimulation provided by a vestibular prosthesis," *IEEE Trans. Biomed. Eng.*, vol. 53, no. 11, pp. 2362-2372, Nov. 2006.

[6] D. M. Merfeld, C. Haburcakova, W. Gong, and R. F. Lewis, "Chronic vestibulo-ocular reflexes evoked by a vestibular prosthesis," *IEEE Trans. Biomed. Eng.*, vol. 54, no. 6, Jun. 2007.

[7] W. Gong, C. Haburcakova, and D. M. Merfeld, "Vestibulo-ocular responses evoked via bilateral electrical stimulation of the lateral semicircular canals," *IEEE Trans. Biomed. Eng.*, vol. 55, no. 11, Nov. 2008.

[8] C. C. Della Santina, A. A. Migliaccio, and A. H. Patel, "A multichannel semicircular canal neural prosthesis using electrical stimulation to restore 3-D vestibular sensation," *IEEE Trans. Biomed. Eng.*, vol. 54, no. 6, pp. 1016-1030, Jun. 2007.

[9] N. Y. Kiang and E. C. Moxon, "Physiological considerations in artificial stimulation of the inner ear," Ann. Otol. Rhinol. Laryngol. vol. 81, no. 5, pp. 714-730, Oct. 1972.

[10] M. A. Saginaw, W. Gong, C. Haburcakova, and D. M. Merfeld, "Angular Vestibulo-Ocular Reflex Above 100 Hz Elicited by Electrical Stimulation of the Vestibular Peripheral Nerve. I. Responses in the Squirrel Monkey," *J. Neurophys.*, to be submitted 2009.

[11] S. J. Judge, B. J. Richmond, and F. C. Chu, "Implantation of magnetic search coils for measurement of eye position: an improved method," *Vis. Res.*, vol. 20, no. 6, pp. 535-538, 1980.

[12] G. D. Paige, "Vestibuloocular reflex and its interactions with visual following mechanisms in the squirrel monkey. II. Response characteristics and plasticity following unilateral inactivation of horizontal canal," J. Neurophys., vol. 49, no. 1, pp. 152-168, 1983.
[13] D. M. Lasker, D. D. Backous, A. Lysakowski, G. L. Davis, and L. B. Minor, "Horizontal vestibuloocular reflex evoked by high-acceleration rotations in the squirrel monkey. II. Responses after canal plugging," *J. Neurophysiol.* vol. 82, no. 3, pp. 1271-1285, 1999.
[14] B. Silveira, Jenks Vestibular Physiology Laboratory, Boston MA, private communication, 2009.
[15] T. L. Babb, H. V. Soper, J. P. Lieb, W. J. Brown, C. A. Ottino, P. H. Crandall, "Electrophysiological studies of long-term electrical stimulation of the cerebellum in monkeys," *J Neurosurg* vol. 47, pp. 353-365, 1977.
[16] R. K. Shepherd, B. K-H. Franz, G. M. Clark, "The biocompatibility and safety of cochlear prostheses," in *Cochlear Prostheses*, G. M. Clark, Y. T. Tong, and J. F. Patrick, Ed. Edinburgh: Churchill Livingstone, 1990, pp. 69-98.
[17] L. S. Robblee, T. L. Rose, "Electrochemical guidelines for selection of protocols and electrode materials for neural stimulation," in: *Neural Prostheses Fundamental Studies*, W. F. Agnew and D. B. McCreery, Ed. Englewood Cliffs, NJ: Prentice Hall, 1990, pp. 25-66.
[18] D. A. Robinson, "A method of measuring eye movement using a scleral search coil in a magnetic field," *IRE Trans. Bio-Medical Electronics*, vol. 10, no. 4, pp. 137-145, Oct. 1963.
[19] M. A. Saginaw, W. Gong, C. Haburcakova, and D. M. Merfeld, "Angular Vestibulo-Ocular Reflex Above 100 Hz Elicited by Electrical Stimulation of the Vestibular Peripheral Nerve. II. Responses in the Guinea Pig," *J. Neurophys.*, to be submitted 2009.
[20] S. Martinez-Conde, S. L. Macknik, and D. H. Hubel, "The role of fixational eye movements in visual perception," *Nature Reviews Neuroscience*, vol. 5. pp. 229-240, Mar. 2004.
[21] M. Yanoff and J. S. Duker, ed., *Ophthalmology, Second Edition*, Mosby, St. Louis, Part 2: Optics and refraction, Chapter 4: Visible light, pp. 33, 2004.
[22] ibid., Chapter 9: Optics of the normal eye, pp. 61.
[23] ibid., Chapter 9: Optics of the normal eye, pp. 66.
[24] R. J. Leigh and D. S. Zee, *The Neurology of Eye Movements*, Oxford, Part 1: The properties and neural substrate of eye movements, Chapter 4: Smooth pursuit and visual fixation, pp. 189, 2006.
[25] E. Kandel, J. Schwartz, and T. Jessell. *Principles of Neural Science, Fourth Edition*. McGraw-Hill Medical, New York, Part IX: Language, Thought, Mood, Learning, and Memory, Chapter 62: Learning and Memory.
[26] ibid, Part IV: Movement, Chapter 41: Posture, pp. 825.
[27] J. H. Courjon, W. Precht, and D. W. Sirkin, "Vestibular nerve and nuclei unit responses and eye movement responses to repetitive galvanic stimulation of the labyrinth in the rat," Exp. Brain Res., vol. 66, no. 1, pp. 41-48, Mar. 1987.
[28] M. A. Saginaw, "Eye movement studies with a vestibular prosthesis," Ph.D. dissertation, Dept. Elect. Eng. and Comp. Sci., MIT, Cambridge MA, 2010.

Michael A. Saginaw (M'96) was born in New York City and spent most of childhood in Maryland. He completed a Bachelor of Science in electrical engineering at MIT in Cambridge, MA, USA, in 1996; and a Master of Engineering in electrical engineering and computer science at MIT in 1997.

He was an Intern and then a Member of Technical Staff in the satellite modem group at COMSAT Laboratories in Clarksburg Maryland, simulating, programming, and demonstrating a real-time FFT-based multicarrier demultiplexer. He is currently a Graduate Student pursuing a Ph.D. in electrical engineering at MIT. Research interests include vestibular neural electrical prostheses and induced high frequency eye movements.

Mr. Saginaw is a student member of IEEE and Society for Neuroscience.

Wangsong Gong received a B.Sc. degree in physiology from Peking University, China, in 1983. He studied at the Xi'an Jiaotong University, China, in a non-degree granting biomedical engineering program from 1983 to 1985. He received a M.Sc. degree in electrical engineering from Northeastern University, Boston MA, in 2005.

From 1985 to 1997, he was a researcher at the Institute of Biomedical Engineering, Chinese Academy of Medical Sciences, China. He is currently an Engineer at Massachusetts Eye and Ear Infirmary, Boston, MA, and a Research Fellow at Harvard Medical School. He is conducting research on vestibular responses to electrical stimulation, and working on the development of neural vestibular prostheses.

Mr. Gong is a member of the Biomedical Engineering Society, and the Society for Neuroscience.

Csilla Haburcakova was born in Kralovsky Chlmec, Slovakia. She received a diploma in general biology at Comenius University, Bratislava in 1998.

From 1998 to 2001 she was working as a junior researcher at Institute of Normal and Pathological Physiology, Slovak Academy of Science, Bratislava, where she also completed her PhD. From 1997 to 1999 she was working as a research fellow in Department of Neurology, Klinikum Grosshadern, Munich, Germany. Currently she is working at Massachusetts Eye and Ear Infirmary, Boston, MA, as a Research Specialist and a Research Fellow at Harvard Medical School. Her research interest focuses on development of a neural vestibular prosthesis and its use in the animals and patients with vestibular disorders.

She is a member of the Society for Neuroscience.

Daniel M. Merfeld (M'91) was born in Wisconsin; he received a Bachelors of Science in Mechanical Engineering (B.S.M.E.) from the University of Wisconsin – Madison in 1982. He then earned a Masters of Science in Engineering (M.S.E.) from Princeton University in 1985 and a Ph.D. in bioengineering from the Massachusetts Institute of Technology (MIT), Cambridge MA, in 1990.

Shortly after his graduation, he joined the Research Staff at MIT and directed the vestibular research activities on two Spacelab Life Sciences (SLS) missions – SLS-1 and SLS-2; he was the Acting PI for the international team performing vestibular investigations on the

SLS-2 mission. In 1995, he began working as a Scientist at the Neurological Sciences Institute in Portland OR. In 1999, he joined the Harvard Medical School faculty as an Associate Professor of Otology and Laryngology and founded the Jenks Vestibular Physiology Laboratory at the Massachusetts Eye and Ear Infirmary, which he now directs. He is also a faculty member at the Harvard-MIT Division of Health Sciences and Technology (HST). Dr. Merfeld received the 1995 Whitaker Young Investigator award from the Biomedical Engineering Society.

He is a member of the Association for Research in Otolaryngology, the Barany Society, the Biomedical Engineering Society, the American Physiological Society, and the Society for Neuroscience. He studies sensory processing of vestibular cues and sensorimotor integration, through the use of physiological and psychophysical measures as well as computational neuroscience techniques such as dynamic systems modeling. Current work focuses on the development of a neural vestibular prosthesis for patients suffering disorders of the peripheral vestibular system. Separate, though related, research focuses on how the nervous system adapts to novel sensory stimuli and how it resolves ambiguous or conflicting sensory information. He is also working to develop clinical tests of vestibular function.

Chapter 5. Conclusions

This thesis has explored the effects of electrical stimulation of the vestibular peripheral nerve on eye movements in squirrel monkeys and guinea pigs. By using electrical stimulation, the angular vestibulo-ocular reflex (VOR) was characterized at frequencies where it is difficult to provide spectrally controlled physical rotation. The discrete Fourier transform was used to analyze eye movements and reveal spectral peaks. These were used to obtain frequency responses and characterize the vestibulo-ocular reflex (VOR) at frequencies substantially higher than have been studied previously. The frequency responses were interpreted in terms of a fourth order linear system model of central processing and the oculomotor plant. Since the VOR is found at frequencies well above 100 Hz, eye movements at the stimulation pulse rate were studied to investigate whether they might cause visual blurring.

Main Contributions

The VOR was characterized at high frequencies, and eye movements at the prosthesis pulse frequency were studied. There were five main findings:

- High Frequency VOR Magnitude Response: The VOR in response to peripheral electric stimulation was characterized from 1.5 to 701 Hz in the squirrel monkey, and from 1.5 to 293 Hz in the guinea pig. In the squirrel monkey the magnitude response was fairly flat up to 5 Hz, fell until 20 Hz, rose to a peak near 140 Hz, and then rolled off. Control tests confirmed that up to 267 Hz, the response was physiological, rather than artifactual. A similar overall shape was found for the guinea pig magnitude response. It was fairly flat up to 8 Hz, rose to a peak near 50 Hz, and then fell off. It was found up to 151 Hz.
- High Frequency VOR Phase Response: The phase response was characterized over the same frequency range. It was very consistent with a pure delay of 4 ms in both the squirrel monkey and the guinea pig.
- Modeling: Linear system modeling of the oculomotor plant and central processing was used to interpret the VOR response. Damping elements in the physical model generate strongly low-pass characteristics for the plant, matching the high frequency roll-off in both squirrel monkeys and guinea pigs.
- Component at Prosthesis Pulse Frequency: Eye movements at the prosthesis pulse frequency were studied. When the pulse rate was 250 pulses/s, there were eye movements at 250 Hz, with a velocity of 8.1 deg/s when stimulation was turned on. However, this reduced with a time constant of 5.0 minutes, and after half an hour the velocity was 1.6 deg/s, corresponding to a 7.3 arcsec peak-to-peak oscillation. That small oscillation would probably not be perceptible for a human using the prosthesis.
- Spectral Extent of Saccades: The spectral impact of saccades and blinks was examined. These non-vestibular eye movements had a substantial effect on the eye movement spectra at low frequencies and some effect up to 160 Hz.

Low Frequency Phase Response

As described above, linear system modeling has been very useful in interpreting the high frequency magnitude and phase responses. Modeling can also be used to understand the phase responses at lower frequencies, but in a tentative way since not as much data are available.

Robinson's fourth order model was from 1964. In 1981 he wrote that the main reason for mechanical modeling is to reveal what data are still needed from physiology experiments. He wrote that input-output transfer function is suitably given by a first or second order model, neither of which predicts a low frequency phase lead. However our data do have a low frequency phase lead, except when using 150 pps stimulation. This was explored in the context of a theory about the neural integrator.

The oculomotor neural integrator is needed to transform eye velocity signals into a motor command that controls eye position (Robinson 1968). Details of the integrator's location and operation have been a subject of research for decades, and the research is ongoing.

The neural integrator can't integrate the value of the spontaneous firing rate, because that would quickly saturate. The integrator must integrate only the fluctuations above and below the spontaneous rate. It has been suggested that the spontaneous rate is subtracted out through lateral inhibition involving commissural networks (Cannon et al. 1983, Arnold and Robinson 1997). Whereas the spontaneous rates on both sides of the head are normally equal, this was not the case in our experiments using unilateral prosthesis stimulation. Therefore, perhaps the neural integrator was not functioning in our experiments. To explore this possibility, the VOR is modeled with and without the integrator.

Figure 5.1 models the signal processing that takes place in the VOR. The head angular velocity, $\dot{H}$, is either sensed by the vestibular periphery or provided by the prosthesis. It is processed centrally, and a command, C, is sent to the oculomotor plant, which is represented by a commonly used model (Robinson 1981) with a single pole with time constant τ, and a fixed delay of T.

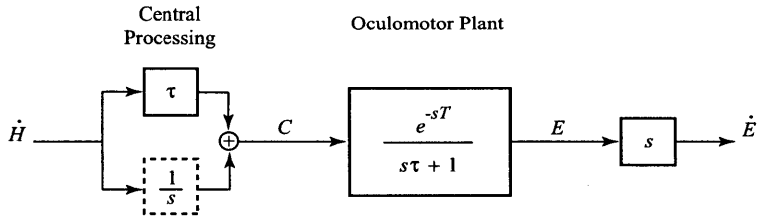

Figure 5.1. Processing of vestibular signals. The head angular velocity, $\dot{H}$, is either sensed by the vestibular system or provided by the prosthesis. In the model, central processing has a gain of τ in the direct path (i.e., the three-neuron arc), which normally works with the neural integrator ("$1/s$") to compensate for the sluggish low-pass character of the oculomotor plant. The integrator is shown in a dotted box because the transfer function is computed with and without the integrator. The output of central processing is sent as a command, C, to the oculomotor plant. The eye position is E. To easily compare the output to the input velocity $\dot{H}$, a differentiator ("s") and the eye velocity, $\dot{E}$, are represented schematically.

If the neural integrator ("1/s") were not present, then the transfer function from the input velocity, $\dot{H}$, to the output eye velocity, $\dot{E}$, would be

$$\frac{\dot{E}(s)}{\dot{H}(s)} = \frac{s\tau}{s\tau + 1} \cdot e^{-sT} \tag{1}$$

Exclusion of the integrator yields a low frequency lead term along with the constant delay. At high frequencies, where central processing is dominated by the direct path, there is little difference between eq. 1 and a pure delay. However at low frequencies, the integrator is expected to dominate central processing, unless it is absent, yielding a phase lead.

Such a phase lead was indeed measured in both the squirrel monkey (chapter 2) and the guinea pig (chapter 3). Figure 5.2A shows data from the squirrel monkey with a biphasic pulse rate of 5000 pulses per second (pps). A similar phase lead was measured in the squirrel monkey with 250 pps (figure 5.2B), in the guinea pig with 598 pps (figure 5.2D), and in the guinea pig with 250 pps (figure 5.2E).

The solid curves in figure 5.2 show the phase of the model. For all panels except panel (C), the phase curve from eq. 1 was used, and a value of 125 ms was used for τ. The plant delay was modeled by T = 5 ms for squirrel monkeys, and by T = 7 ms for guinea pigs.

If the prosthesis biphasic pulse rate were closer to the animal's spontaneous rate, then the neural integrator function might be restored. With the neural integrator functioning, the transfer function would be

$$\frac{\dot{E}(s)}{\dot{H}(s)} = e^{-sT} \tag{2}$$

which does not have a low frequency phase lead.

Experiments were also done using a biphasic pulse rate of 150 pps. For the squirrel monkey, the low frequency phase lead was indeed abolished (figure 5.2C). The biphasic pulse rate of 150 pps was considerably closer to the squirrel monkey's spontaneous rate of 90 spikes/s. Due to variation, approximately 3% of units have a spontaneous rate of 150 spikes/s or higher (Goldberg and Fernandez 1971). Furthermore, for half of each modulation cycle, there was no stimulation, and firing was at the spontaneous rate, so the average firing rate on the stimulated side was 120 spikes/s, which was even closer to the contralateral rate.

When 150 pps was used in the guinea pig, however, there was still a clear low frequency phase lead (figure 5.2F). This may have been due to the fact that the spontaneous rate in guinea pigs is approximately 30-60 spikes/s (Ris and Godaux 1998, Curthoys 1982), which is so far below the unilateral stimulation pulse rate that the neural integrator may not have been functioning. This predicts that the guinea pig low frequency phase lead would also disappear with an even lower prosthesis baseline rate, closer to the guinea pig's resting rate.

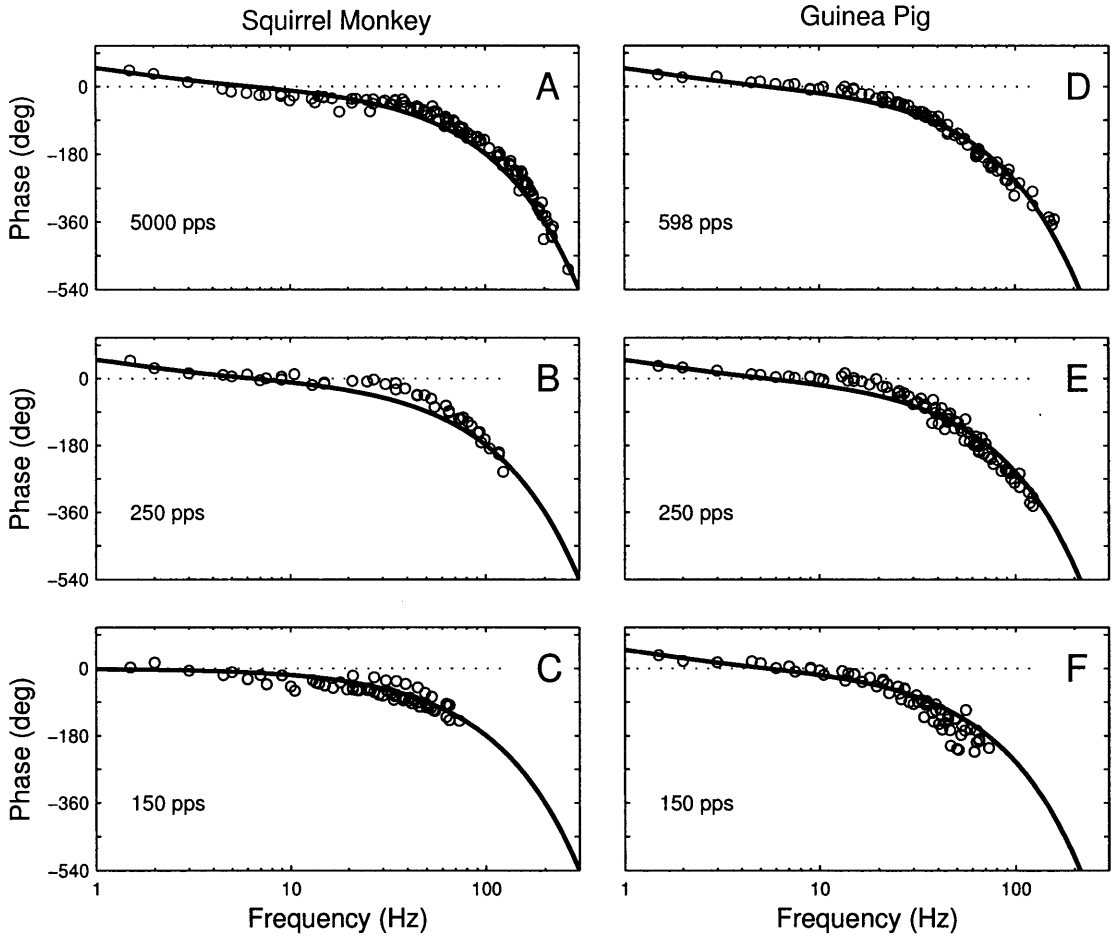

Figure 5.2. Phase responses. All panels show a low frequency phase lead except panel (C), which used a stimulation pulse rate close enough to the species' spontaneous rate (90 spikes/s) that the neural integrator may have been functioning. The prosthesis stimulation pulse rate is displayed in each figure. Solid curves show the theoretical phase. The phase lead term in eq. 1, with τ = 125 ms, was used for all panels except panel (C), which used eq. 2. A delay of T = 5 ms was used for all squirrel monkey data sets; the delay was T = 7 ms for all guinea pig data sets. Panels (A) and (B) show data from monkey "R". Panel "C" shows averages from monkeys "R" and "N" (right ear stimulation). Panels (D) and (E) show averages from guinea pigs "S", "D", and "G". Panel (F) shows averages from guinea pigs "S", "D", and "O".

Speculating further, if the neural integrator requires equal spontaneous rates on both sides of the head, perhaps a major role of the efferent vestibular system is to equalize those rates. Otherwise there might be a discrepancy in the bilateral rates over the long term, interfering with the function of the neural integrator. The function of the efferent vestibular system has remained unclear for a long time. One hypothesis was that the efferent system acts differently for active vs. passive head movements, but this has been rejected (Cullen and Minor 2002). It has been suggested that one role of the efferent system is to equalize the spontaneous rates on both sides of the head (Cullen and Minor 2002), though the connection to the neural integrator has not previously been made. Furthermore, if the efferent system does maintain balance of the spontaneous rates, this could give rise to the Young-Oman time constant, in which even prolonged

acceleration does not elicit prolonged vestibular stimulation (Young and Oman 1969, Goldberg and Fernandez 1971).

Certainly, linear system theory continues to be a valuable tool for understanding physiological data and helping to suggest new interpretations, hypotheses, and experiments.

References

Andrews JC, Koyama S, Li J, Hoffman LF. Vestibular and optokinetic function in the normal guinea pig. *Ann Otol Rhinol Laryngol* 106: 838-847, 1997.

Arnold DB, Robinson DA. The oculomotor integrator: testing of a neural network model. *Exp Brain Res* 113: 57-74, 1997.

Cannon SC, Robinson DA, Shamma S. A proposed neural network for the integrator of the oculomotor system. *Biol Cybern* 49: 127-136, 1983.

Cullen KE, Minor LB. Semicircular canal afferents similarly encode active and passive head-on-body rotations: implications for the role of vestibular efference. *J Neurosci* 22: RC226: 1-7, 2002.

Curthoys IS. The response of primary horizontal semicircular canal neurons in the rat and guinea pig to angular acceleration. *Exp Brain Res* 47: 286-294, 1982.

Goldberg JM, Fernandez C. Physiology of peripheral neurons innervating semicircular canals of the squirrel monkey. I. Resting discharge and response to constant angular accelerations. *J Neurophysiol* 34: 635-660, 1971.

Ris L, Godaux E. Spike discharge regularity of vestibular neurons in labyrinthectomized guinea pigs. *Neurosci Lett* 253: 131-134, 1998.

Robinson DA. Eye movement control in primates. *Science* 161: 1219-1224, 1968.

Young LR, Oman CM. Model of vestibular adaptation to horizontal rotations. *Aerospace Med* 40: 1076-1080, 1969.